

AD _____

Award Number: DAMD17-00-1-0048

TITLE: Structure/Function Studies of the Androgen Receptor
DNA-Binding Region

PRINCIPAL INVESTIGATOR: Fraydoon Rastinejad, Ph.D.

CONTRACTING ORGANIZATION: University of Virginia
Charlottesville, Virginia 22904

REPORT DATE: April 2003

TYPE OF REPORT: Final

PREPARED FOR: U.S. Army Medical Research and Materiel Command
Fort Detrick, Maryland 21702-5012

DISTRIBUTION STATEMENT: Approved for Public Release;
Distribution Unlimited

The views, opinions and/or findings contained in this report are those of the author(s) and should not be construed as an official Department of the Army position, policy or decision unless so designated by other documentation.

20041118 057

REPORT DOCUMENTATION PAGE

Form Approved
OMB No. 074-0188

Public reporting burden for this collection of information is estimated to average 1 hour per response, including the time for reviewing instructions, searching existing data sources, gathering and maintaining the data needed, and completing and reviewing this collection of information. Send comments regarding this burden estimate or any other aspect of this collection of information, including suggestions for reducing this burden to Washington Headquarters Services, Directorate for Information Operations and Reports, 1215 Jefferson Davis Highway, Suite 1204, Arlington, VA 22202-4302, and to the Office of Management and Budget, Paperwork Reduction Project (0704-0188), Washington, DC 20503

1. AGENCY USE ONLY (Leave blank)

2. REPORT DATE

April 2003

3. REPORT TYPE AND DATES COVERED

Final (1 Apr 00 - 31 Mar 03)

4. TITLE AND SUBTITLE

Structure/Function Studies of the Androgen Receptor DNA-Binding Region

5. FUNDING NUMBERS

DAMD17-00-1-0048

6. AUTHOR(S):

Fraydoon Rastinejad, Ph.D.

7. PERFORMING ORGANIZATION NAME(S) AND ADDRESS(ES)

University of Virginia
Charlottesville, Virginia 22904

E-Mail: fr9c@virginia.edu

8. PERFORMING ORGANIZATION
REPORT NUMBER

9. SPONSORING / MONITORING AGENCY NAME(S) AND ADDRESS(ES)

U.S. Army Medical Research and Materiel Command
Fort Detrick, Maryland 21702-5012

10. SPONSORING / MONITORING
AGENCY REPORT NUMBER

11. SUPPLEMENTARY NOTES

Original contains color plates: All DTIC reproductions will be in black and white.

12a. DISTRIBUTION / AVAILABILITY STATEMENT

Approved for Public Release; Distribution Unlimited

12b. DISTRIBUTION CODE

13. Abstract (Maximum 200 Words) (abstract should contain no proprietary or confidential information)

The androgen receptor (AR) regulates the growth and differentiation of prostate cells and is an important drug target for prostate cancer chemotherapy. The research goals associated with this study are to characterize the structural and functional aspects of the AR in order to uncover the potential of its domains, and in particular the DNA-binding domain, as a drug target. In this final report, I discuss the results obtained over the past three years towards characterization of the AR. Among our findings are a) the DNA-binding domain of the androgen receptor and related nuclear receptors act as their nuclear export signals, b) their export is dependent on their binding to the protein calreticulin in the presence of calcium, c) by analogy with our recent crystal structure of EcR-Usp on DNA, a pair of DNA-binding domains are arranged symmetrically as a homodimer with respect to each other and directly on the half-sites of their target DNA, d) the ligand binding domain is analogous to the FXR ligand-binding domain and shares highly related surfaces responsible for DHT binding and coactivator binding.

14. SUBJECT TERMS:

androgen receptor, DNA binding

15. NUMBER OF PAGES

43

16. PRICE CODE

17. SECURITY CLASSIFICATION
OF REPORT

Unclassified

18. SECURITY CLASSIFICATION
OF THIS PAGE

Unclassified

19. SECURITY CLASSIFICATION
OF ABSTRACT

Unclassified

20. LIMITATION OF ABSTRACT

Unlimited

Table of Contents

Cover.....	
SF 298.....	2
Introduction.....	4-5
Body and Key Research Accomplishments	6-11
Reportable Outcomes.....	11
Conclusions.....	12
References.....	--13
Appendices.....	3 manuscripts

Structure-Function Studies of Androgen Receptor DNA Binding Region

INTRODUCTION

The androgen receptor (AR) is a member of the nuclear hormone receptor superfamily, a class of ligand-activated gene-regulatory factors. Nuclear receptors, including AR, regulate gene expression through specific DNA binding sites known as hormone response elements. The nuclear receptors consist of modular domains, including a central and well-conserved region known as the DNA-binding domain (DBD), an un-conserved C-terminal extension known as the hinge region, and a C-terminal portion known as the ligand-binding domain (LBD) [see Figure 1]. The DBD imparts the receptor's entire DNA-binding specificity and selectivity. The LBD allows receptors to bind to ligands and coregulator proteins. The AR is a good drug target for current and future anti-prostate cancer therapy, because it is responsible for the growth and differentiation of the normal and cancerous cells of the prostate.

The DBDs within the nuclear receptor family may be classified into distinct groups based on the geometry of their target DNA binding sites (also known as hormone response elements). Class-I receptors bind to hormone response elements that consist of an inverted (or palindromic) repeat of the hexamer AGGTCA or AGTTCA (see Figure 1). In this group is AR homodimer, the glucocorticoid receptor (GR) homodimer, the mineralocorticoid receptor (MR) homodimer, and the Ecdysone receptor-Ultraspirlacle (EcR-Usp) heterodimer. Class-II receptors are those that bind to direct repeats of the same hexameric sequences. These members are generally the receptors that form heterodimers with the retinoid-X-receptor (RXR), such as the thyroid hormone receptor (TR), the vitamin D receptor (VDR), and the all-trans retinoic acid receptor (RAR). Our lab has previously characterized a number of new crystal structures for the type-II receptors in which the DBDs of RXR and its partners were assembled on direct-repeat hormone response elements.

Prior to starting the studies in this proposal, the DBDs had been

viewed as having only one type of function, that of targeting the receptors to their correct DNA sites. Therefore, we sought to investigate other possible functions associated with the DBDs, and uncovered a previously unknown role in nuclear export. We also characterized and reported on the other protein players responsible for the export of AR. These studies have produced significant impact on the field, as there was no previous knowledge available regarding how nuclear receptors exit the nucleus.

In terms of the characterizing the structures of the DBDs, we have been pursuing the goal of providing a detailed crystallographic model of how the AR DBD and in general the other class-I receptors are able to form homodimers on their consensus type response element. Due to intractable diffraction limitations with respect to the AR complex, we instead pushed forward and determined another class-I receptor/DNA complex structure that we know shares all of the essential hallmarks associated with the AR/DNA complex. In addition, we went beyond all of the aims in the original proposal by attempting to extend the known structural features reported by another group on the AR ligand-binding domain (LBD). In that structure, there was no coactivator present in

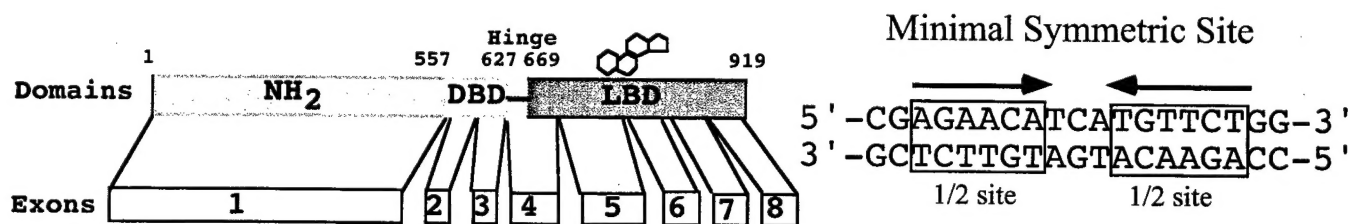


Figure 1: The domain structure of the androgen receptor and the inverted-repeat geometry and sequence of its hormone response element (DNA-binding site).

the crystal structure and thus no lessons as to how a steroidal molecule activates the AR. Again, by focus on a highly related steroid receptor, FXR, we were able to gain important new structural insights as to how steroids are likely to reshape the LBD configuration to recruit the binding of LXXLL motifs associated with the p160 protein of coactivators.

BODY and Key Research Accomplishments

DNA-Binding Domain Functional Characterization

(Appendix-1, Black et al., 2001) contains our first reported findings. In this study, we were able to identify the location of the nuclear export signals (NES) within the AR, and also within closely related receptors and to characterize their functions related to their nuclear export pathway. We found that the core DBD region of AR and this receptor, which are closely homologous to each other but unrelated to any known NES, are the regions that are directly responsible for their nuclear export. Mutational analysis revealed that a 15 amino acid sequence between the two zinc binding loops in the DBD confers nuclear export to a green-fluorescence protein construct, and alanine-scanning mutagenesis was used to identify the residues within this sequence that are critical for export. We went on to test and show that the DBDs from ten different nuclear receptors all function as the same export signal. Our findings guided us to propose that NLS-mediated import and DBD-mediated export define a shuttling cycle that integrates the compartmentalization and activity of nuclear receptors.

(Appendix-2, Holaska et al, 2002) contains our second published report which describes how we have recently characterized a pathway for nuclear export of the nuclear receptors in mammalian cells. This pathway involves the $\text{Ca}(2+)$ -binding protein calreticulin (CRT), which directly contacts the DNA binding domain (DBD) of AR, and related receptors and allows their transport from the nucleus to cytoplasm. We examined a role of $\text{Ca}(2+)$ in CRT-dependent export of these receptors. Removing $\text{Ca}(2+)$ from CRT inhibits the stimulation of the nuclear export, an effect due to the failure of CRT to bind the DBD of these receptors. These effects are reversible, when there is a restoration of $\text{Ca}(2+)$. Depletion of intracellular $\text{Ca}(2+)$ inhibits receptor export in intact cells under conditions that do not inhibit other nuclear transport pathways. We also found that the Ran GTPase is

not required for GR export. It appears that the nuclear export pathway used by steroid hormone receptors are most likely distinct from the Crm1 pathway. Our data has been leading us to consider whether signaling events that increase Ca^{2+} could positively regulate CRT and inhibit GR function through nuclear export.

DNA-Binding Domain Structural Characterization

We obtained crystals of the AR-DBD/DNA which were small and generally poorly diffracting (see Figure 2). To improve the quality of the crystals and to obtain a high-resolution structure, we attempted a series of different approaches. First, we made a series of new protein expression constructs. The rationale was that perhaps additional sequences C-terminal to the core DBD would enhance DNA binding and stabilize the complex and the crystal lattice. Five different constructs were made in our laboratory, each with a common N-terminal (His)₆ tag for purification. Each of the five new constructs contained the core DBD region, plus 0, 10, 20, 30, 41 residues of hinge regions, respectively. The purification involved an initial Ni-NTA column followed by a S-column (cation exchange). These constructs are cloned into pET16b vector, and expressed in BL21DE3 strain. A Ni-NTA column and an S column are used to purify the proteins.

In each case, we did obtain good protein yields, and could purify the AR-DBDs effectively as described above (see Figure 4 for an example). Moreover, we tested and attempted to confirm that each of these AR DBD polypeptides retained the ability to bind DNA (see Figure 5). A surprising finding was that in essentially all cases, the binding to an Androgen Response element (ARE) could be competed out with excess non-specific DNA (Figure 5). This was disturbing and suggested that the reason we may have been unable to get well-



Figure 2: Preliminary crystals of the AR-DBD in complex with a consensus inverted-repeat-3 DNA diffracted poorly when tested at home with a Rigaku-RU2HR X-ray generator B: crystals of the 'extended' complex involving the 27 base pair natural (probasin gene) AR response element, with AR DBD with a longer hinge region also diffracted poorly.

diffracting crystals was the AR-DBD was binding the synthetic DNA in the crystallization mixture using a non-specific binding mode.

We then set out to vary the type of DNA used in the crystallization with the hope that we could identify a more suitable binding site which would promote very tight and specific binding with the AR-DBD. In particular, we examined the probasin gene which contains more than one AR binding element. Using additional DNA synthetic constructs corresponding to these AREs, we again were unable to show very strong and specific binding which was not easily competed out with non-specific DNA.

These efforts to produce stable protein-DNA complexes of AR continued without much success over the first two years. In the past year, we switched our strategy by focusing instead on another steroid receptor DBD /DNA complex which we felt shared most of the hallmarks that are associated with AR. This work has recently led to our determination and refinement of a high resolution (2.4 Å) crystal structure of the EcR-Usp heterodimer bound to a symmetric DNA site related to the Androgen-response elements.

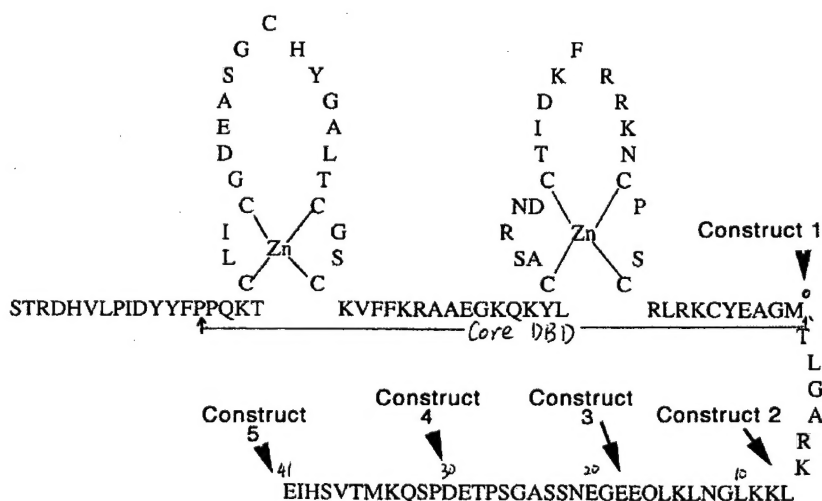


Figure 3: AR-DBD protein constructs made to improve crystal quality and diffraction.

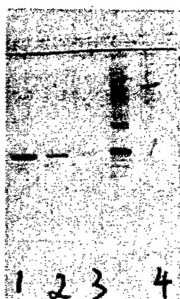


Figure 4: typical protein purification of AR-DBDs. Construct 5 is purified from a Pharmacia Fast-S column. Lanes 1-3 show the peak fractions eluted with 300 mM NaCl containing buffer. Lane 4 shows molecular weight markers.

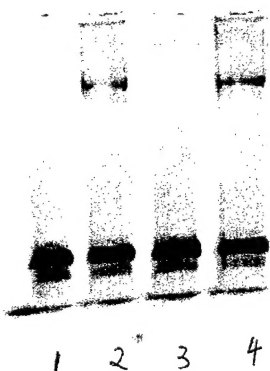


Figure 5: Gel shift analysis of the binding of Construct 5 (see Figures 3 and 4) to DNA. Lane 1: Free DNA (ARE2; 40nM); lane 2: DNA: AR-DB at ratio of 1: 15 (mol ratio) lane 3: Same as lane 2 but with 2uM poly dIdC; lane 4: ARE DNA to AR-DBD ratio of 1: 30.

Figure 6 shows our recently determined crystal structure of the EcR-Usp complex bound to a synthetic symmetric DNA element – having the same half-site geometry as a consensus ARE. The following lessons learned from the analysis of this complex are expected to be fully shared with the AR DBD complex on its symmetric element. First, the DBDs use an alpha-helix to engage the major groove of their core hexameric site. These portion of the receptor DBD, (“the recognition helix”) is nearly identical in amino-acid sequence between the AR, Usp and EcR. Second, the subunits form a dimeric arrangement in which the Zn-II loops of the two subunits form their protein-protein interactions, and these are likely to be the same regions used by the AR. Finally, the subunits cooperate to bind their element by using the inter-protein contacts so that the binding of one subunit stabilizes and enhances the effectiveness of the binding of the second subunit. We are currently initiating a

mutagenesis study in which we are replacing the hinge regions (of various size) from EcR with their corresponding sequences from AR. We would like to re-examine additional crystal structures of these EcR(mut)-Usp/DNA to assess the roles of the AR hinge regions, which we are otherwise unable to do in the context of an AR-DBD crystal structure.

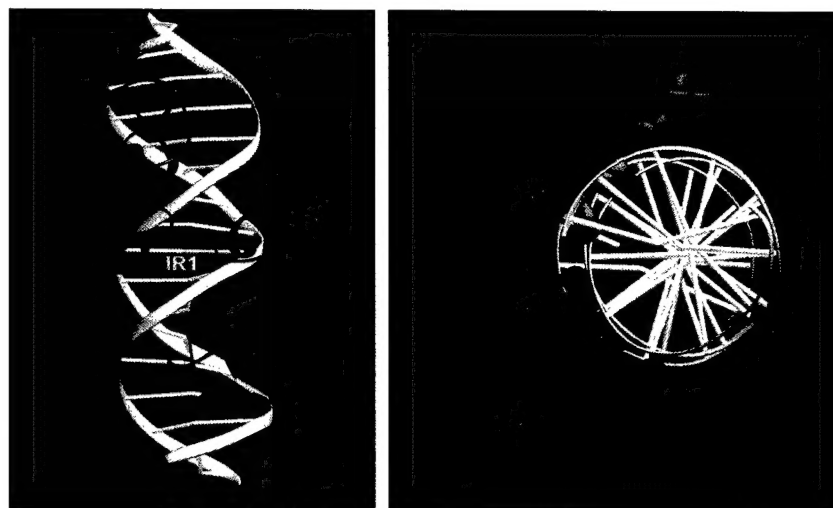


Figure 6: Two views of the EcR-Usp DNA-binding complex on their symmetric repeat DNA site. The major determinants for DNA recognition and protein dimerization are likely to be closely shared with the AR. The green spheres show the positions of the two Zn atoms, which nucleate a Zn-I and a Zn-II loop.

Understanding additional Structural and Functional Attributes of AR

While we were carrying out our work on the DBD portion of the AR, we noticed that some related structural work on the distinct LBD portion was reported by another group (ref 1). That study showed how androgens bind to the pocket of the AR-LBD. However, there were many unanswered questions. Among these was how the ligand alters the conformation so that the LBD can recruit p160 coactivators to bind to its surface. The binding of p160 coactivators to AR is a direct functional consequence of steroid activation and is required for AR function. While it had been known that the p160 proteins rely on discrete LXXLL motifs (where L is leucine and X is any residue) within their sequence to bind to steroid receptors, there was little structural insight on how this was actually done.

Therefore, we studied the LBD of the nuclear receptor FXR, which also binds to steroids like the AR. We recently reported (see Mi et al, 2003 in the appendix) the structure of this LBD bound to both its steroidal ligand and to p160 protein derived LXXLL motifs. In the paper, we describe the similarities with the AR as well as the mechanism of how helix-12 in these receptors can be forced in an agonist conformation that supports LXXLL sequence binding on the surface of the LBD. New and unexpected were the findings that two LXXLL motifs could bind simultaneously to the surface of the FXR by forming cooperative interactions with each other and the LBD. These results are now prompting us to examine, using a mutagenesis study, whether the AR LBD can also accommodate the binding of two p160 motifs in the presence of ligands.

Reportable Outcomes

A) Five *E. coli* over-expression clones for producing AR-DBD.

B) Publications and Manuscripts Pending Publication:

- i) Black, B.E., Holaska, J.M, Rastinejad, F., Paschal, B.M.
DNA binding domains in diverse nuclear receptors function as nuclear export signals. *Current Biology*, 11: 1749-1758 (2001).
- ii) Holaska, J.M., Black, B.E., Rastinejad, F., Paschal, B.M.
Ca²⁺ regulates the nuclear export activity of calreticulin. *Mol. Cell Biol.* 22:6286-97 (2002)
- iii) Devarakonda, S., Harp, J.M., Kim, Y., and Rastinejad, F.
Crystal structure of the EcR-Usp DNA binding complex and its relationship to the other steroid receptors. (Manuscript in preparation, 2003)
- iv) Mi, L, Devarakonda, S, Harp, J.M., Han, Q., Pellicciari, R. Willson, T., Khorasanizadeh, S., Rastinejad F.
Structural basis for bile acid binding and activation of the nuclear receptor FXR.
Molecular Cell, 11:1093-11:00. (2003).

Conclusions:

The past three years have seen exciting results from our laboratory in understanding the structure and function of AR domains. We have characterized an important and previously unknown function associated with the DNA-binding domain. While our structural work on the AR/DNA complex has been difficult, we were able to solve the corresponding structure of another, highly related DBD/DNA complex that shows the essential hallmarks associated with the AR protein. Finally, we have also studied the LBD regions of steroid receptors and have uncovered new mechanisms by which the AR and related members of the superfamily are activated by their steroidal ligands to bind to p160 coactivator proteins.

Appendix 1 and 2 and 3:

Publications:

Black, B.E., Holaska, J.M., Rastinejad, F., Paschal, B.M.
DNA binding domains in diverse nuclear receptors function as nuclear export signals. *Current Biology*, 11: 1749-1758 (2001).

Holaska, J.M., Black, B.E., Rastinejad, F., Paschal, B.M.
Ca²⁺ regulates the nuclear export activity of calreticulin.
Mol. Cell Biol. 22:6286-97 (2002).

Mi, L., Devarakonda, S., Harp, J.M., Han, Q., Pellicciari, R.
Willson, T., Khorasanizadeh, S., Rastinejad F.
Structural basis for bile acid binding and activation of the nuclear receptor FXR.
Molecular Cell, 11:1093-11:00. (2003).

Individuals Supported by this grant

Fraydoon Rastinejad, PI

Qiang Zhao (Research Associate) involved with AR-DBD/DNA crystallizaion

Christine Wright (Research Professor), working with Qiang Zhao on AR protein crystallization

Srikripa Devarkonda (Biophysics Graduate Student) responsible for determining the EcR-Usp Complex

LiZhi Mi (Biophysics Graduate Student) Responsible for understanding how p160 proteins bind to steroid receptor LBDs

References:

- 1) Matias PM, Donner P, Coelho R, Thomaz M, Peixoto C, Macedo S, Otto N, Joschko S, Scholz P, Wegg A, Basler S, Schafer M, Egner U, Carrondo MA. Structural evidence for ligand specificity in the binding domain of the human androgen receptor. Implications for pathogenic gene mutations. J Biol Chem. 2000; 275(34):26164-71.

DNA binding domains in diverse nuclear receptors function as nuclear export signals

Ben E. Black^{*†‡}, James M. Holaska^{*}, Fraydoon Rastinejad^{†§} and Bryce M. Paschal^{*†‡}

Background: The nuclear receptor superfamily of transcription factors directs gene expression through DNA sequence-specific interactions with target genes. Nuclear import of these receptors involves recognition of a nuclear localization signal (NLS) by importins, which mediate translocation into the nucleus. Nuclear receptors lack a leucine-rich nuclear export signal (NES), and export is insensitive to leptomycin B, indicating that nuclear export is not mediated by Crm1.

Results: We set out to define the NES in the glucocorticoid receptor (GR) and to characterize the export pathway. We found that the 69 amino acid DNA binding domain (DBD) of GR, which is unrelated to any known NES, is necessary and sufficient for export. Mutational analysis revealed that a 15 amino acid sequence between the two zinc binding loops in the GR-DBD confers nuclear export to a GFP reporter protein, and alanine-scanning mutagenesis was used to identify the residues within this sequence that are critical for export. The DBD is highly related (41%–88% identity) in steroid, nonsteroid, and orphan nuclear receptors, and we found that the DBDs from ten different nuclear receptors all function as export signals. DBD-dependent nuclear export is saturable, and prolonged nuclear localization of the GR increases its transcriptional activity.

Conclusions: Multiple members of the nuclear receptor superfamily use a common pathway to exit the nucleus. We propose that NLS-mediated import and DBD-mediated export define a shuttling cycle that integrates the compartmentalization and activity of nuclear receptors.

Background

Nuclear receptors contain a structurally conserved DBD that contacts the respective DNA response element within enhancers of target genes [1–3]. Ligand-occupied nuclear receptors interact with transcriptional coactivators, whereas ligand-free nuclear receptors interact with transcriptional repressors. Ligand binding has, in addition, a profound influence on the subcellular distribution of certain nuclear receptors [4]. Glucocorticoid binding to GR induces receptor translocation from the cytoplasm to the nucleus [5], and androgen induces translocation of the androgen receptor (AR) to the nucleus as well [6]. Nuclear import occurs because ligand binding to nuclear receptors releases chaperones and exposes one or more NLSs. GR contains two ligand-regulated NLSs, one of which is located in the hinge region adjacent to the DBD [5]. The NLS is, in turn, recognized by nuclear import factors that facilitate translocation of the nuclear receptor through the nuclear pore complex and delivery to the nucleoplasm [7, 8].

Certain nuclear receptors have also been shown to undergo export from the nucleus. Hormone withdrawal from

cells induces the cytoplasmic accumulation of GR and AR [6, 9]. Moreover, in the presence of ligand where nuclear receptors appear constitutively nuclear, GR, AR, thyroid hormone receptor (TR), and the progesterone receptor (PR) are rapidly shuttling between the nucleus and cytoplasm [6, 10–13]. Because the sizes of these and other nuclear receptors (43–90 kDa) exceeds the molecular weight cutoff for simple diffusion through the nuclear pore, it has been inferred that nuclear export of nuclear receptors is a facilitated process. The balance of nuclear import and export could be an important mechanism for regulating the transactivation potential of nuclear receptors. Indeed, selective nuclear localization of factors involved in signal transduction and transcription has emerged as an important regulatory step in several biological pathways [14].

The best-characterized nuclear export pathway uses Crm1 as a receptor for proteins that contain a leucine-rich NES. Nuclear receptors such as GR, AR, TR, and PR do not, however, contain a leucine-rich NES, suggesting that these proteins are not transport substrates for Crm1. This view is corroborated by the observation that the Crm1-

Addresses: ^{*}Center for Cell Signaling, [†]Department of Biochemistry and Molecular Genetics, [‡]Cell and Molecular Biology Program, and [§]Department of Pharmacology, University of Virginia, Charlottesville, Virginia 22908, USA.

Correspondence: Bryce M. Paschal
E-mail: paschal@virginia.edu

Received: 13 August 2001
Revised: 11 September 2001
Accepted: 27 September 2001

Published: 13 November 2001

Current Biology 2001, 11:1749–1758

0960-9822/01/\$ – see front matter
© 2001 Elsevier Science Ltd. All rights reserved.

specific inhibitor leptomycin B does not inhibit nuclear export of GR, PR, AR, or TR in mammalian cells [9, 13, 15–17]. Recent insight into how nuclear receptors may exit the nucleus came from a biochemical screen for nuclear export factors present in extracts prepared from mammalian cells [17]. The calcium binding protein calreticulin (CRT) was identified as a factor that stimulates nuclear export of proteins that contain a leucine-rich NES [17]. The previous link between CRT and downregulation of GR, AR, all-trans retinoic acid receptor (RAR), and vitamin D receptor (VDR) transcriptional activity [18–20] suggested a potential role in the export of nuclear receptors as well, despite the absence of a leucine-rich NES in these proteins. Recombinant CRT stimulates nuclear export of GR in permeabilized cell assays, and GR export, which is deficient in *crt*^{-/-} cells, can be complemented by back-transfecting CRT [17].

Here we characterize the signal for nuclear export of GR, which is contained within its DBD. Moreover, the DBD functions as the export signal in multiple steroid, nonsteroid, and orphan nuclear receptor family members. The DBD export pathway is saturable, indicating that nuclear receptors compete for a limited number of soluble transport factors, NPC binding sites, or both. Overexpression of the VDR DBD inhibits GR export and results in an elevated transcriptional response of GR to dexamethasone (Dex). Thus, the DBD export pathway contributes to the regulation of GR and probably other nuclear receptors through a nuclear transport-based mechanism.

Results

The DBD of GR contains the NES

The DBD of GR can be incorporated into a green fluorescent protein (GFP) reporter and can function as an NES when expressed in cultured cells [17]. The conserved sequence and structure of the DBD in different nuclear receptors (Figure 1a,b) led us to hypothesize that the DBD is widely used as an export signal. To address this hypothesis, we first mapped the molecular determinants of the 69 amino acid GR DBD that are necessary for nuclear export by using a GFP reporter that undergoes ligand-dependent nuclear import (Figure 1c). Following ligand removal from the cell culture media, the distribution of the GFP reporter was recorded at 0, 2, 4, and 6 hr by fluorescence microscopy. We found that cysteine to alanine mutations that disrupt the zinc binding loops and abolish DNA binding only slightly inhibited nuclear export of the GFP reporter (C424A and C463A; Figure 2). This suggested that nuclear export might instead rely on the DNA recognition helix that is situated between the two zinc binding loops. Indeed, a GFP reporter that contained only 15 amino acids of the GR DBD (442–456) underwent translocation from the nucleus to the cytoplasm. Although the zinc binding loops of nuclear receptors do not contain information that is critical for export

specified by the DBD, there may be a contribution to the DBD structure that augments recognition of the signal by the export machinery.

Alanine-scanning mutagenesis of the DNA recognition helix between the loops revealed that a pair of phenylalanines is critical for the export function of the DBD (FF→AA; Figure 2). Mutating other pairs of amino acids between the zinc fingers (KR→AA, VE→AA, and YL→AA) impaired the nuclear export function of the GR DBD to a lesser degree (2 and 4 hr time points). In contrast, other mutations (KV→AA, GQ→AA, and HN→AA) had no effect on the export activity of the GR DBD. Our data show that amino acids between the two zinc binding loops, which include part of the DNA recognition helix, contain the NES of GR.

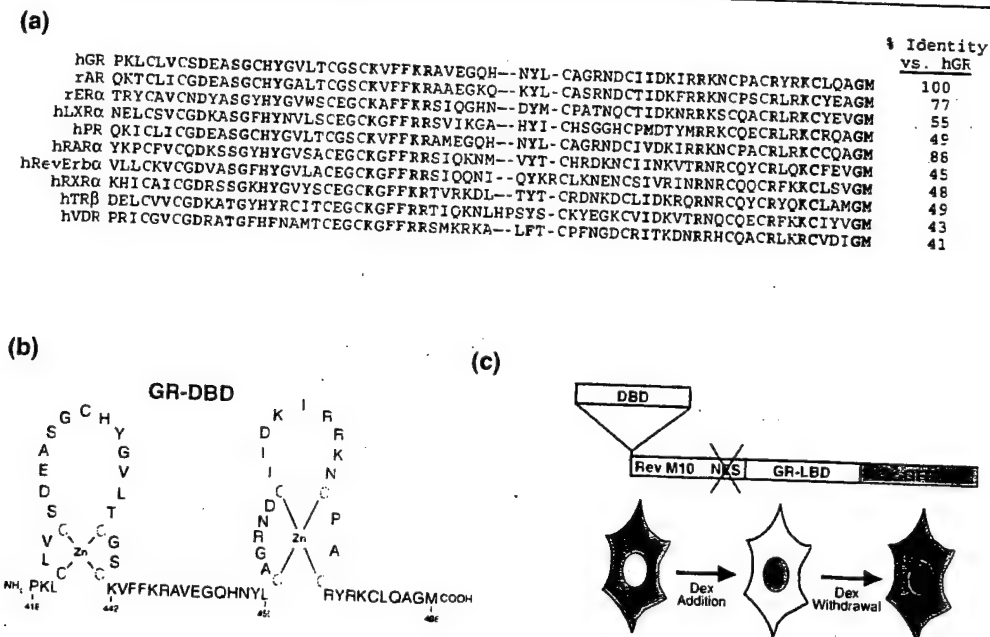
Steroid, nonsteroid, and orphan receptors use a common export pathway

Our finding that the GR DBD contains the NES appeared significant in light of the structural conservation of the DBD among nuclear receptors. The GR DBD is at least 40% identical to the sequences of DBDs from nine different nuclear receptors included in our analysis (Figure 1a). Moreover, every member of the nuclear receptor superfamily that has been identified to date contains a pair of phenylalanines that are located at the same position relative to phenylalanines within the GR DBD. This led us to hypothesize that the DBDs from diverse nuclear receptors can function as an NES. We tested this hypothesis by analyzing the export activity of DBDs from steroid, nonsteroid, and orphan nuclear receptors. We found that nuclear export of the GFP reporter was conferred by the DBD derived from AR, estrogen receptor (ER), liver X receptor (LXR), PR, RAR, RevErb, retinoid X receptor (RXR), TR, and VDR (Figure 3). Nuclear export was not conferred by the DBD derived from GATA1, a transcription factor that, like the nuclear receptors, contains two zinc binding loops in its DBD [21]. GATA1 is not, however, a member of the nuclear receptor superfamily based on sequence or structure. Thus, our data identify the DBD of nuclear receptors as a new type of NES. The DBD does not contain a leucine-rich NES that is recognized by the export receptor Crm1, which may explain why nuclear export of GR, PR, TR, and AR are insensitive to leptomycin B [9, 13, 15–17].

Mutations in the DBD block nucleocytoplasmic shuttling of nuclear receptors

Our experiments demonstrated that the DBD is sufficient to mediate nuclear export in the context of the GFP reporter. To determine whether the DBD is necessary for export in the context of the receptor, we examined nucleocytoplasmic shuttling of full-length, wild-type (wt) GR, AR, and RAR, and of mutant forms of these receptors that were predicted to be deficient for export. We designed a modified-shuttling assay that, in a heterokaryon

Figure 1



Conserved structure of the DBD and assay for nuclear export activity. (a) Alignment of DBDs from nuclear receptors used in this study and the percent identity to the DBD of human GR. Highly conserved residues (bold) including the cysteines that coordinate zinc binding (green) and the pair of phenylalanines that are present in the DNA recognition helix of all nuclear receptors (red) are indicated. (b) Diagram of the GR DBD showing the position of the pair of phenylalanines relative to the zinc binding loops. (c) Features of the

GFP reporter and two-step assay for nuclear export in vivo. The vector encodes a mutant form of Rev (M10) that contains a nonfunctional NES fused to the ligand binding domain (LBD) of GR and GFP. Dex induces nuclear import of the GFP reporter, which remains nuclear after Dex withdrawal because the reporter lacks a functional NES. In-frame fusion of a DBD to the N terminus of the GFP reporter restores nuclear export activity.

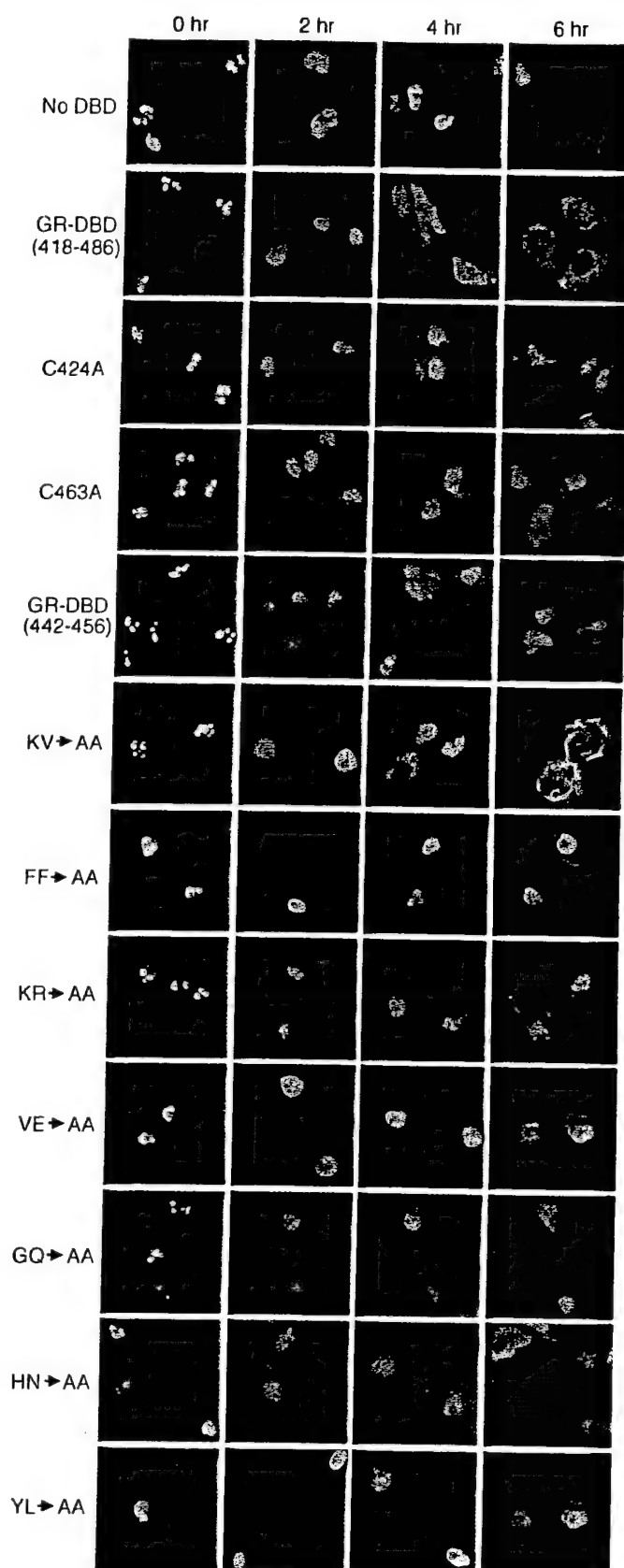
fusion, scores nuclear export from a donor nucleus and nuclear import into an acceptor nucleus. Prior to fusion (Figure 4a, upper panels), the donor cells (human) were transfected with GFP fusions of the receptors and treated with the appropriate ligand to induce nuclear import. The acceptor cells (mouse) were labeled with a CellTracker dye that, following its uptake, is converted to a membrane impermeant form in the cytoplasm. After fusion (Figure 4a, lower panels), the cytoplasm of the heterokaryon fluoresces red, and the GFP fusion (green) containing full-length GR equilibrates between the human and mouse nuclei because it undergoes shuttling, as previously shown [11]. The GFP reporter used in prior experiments to characterize the DBD (Figure 1c) undergoes nuclear import, but fails to undergo export and equilibrate between nuclei in the heterokaryon because it lacks a functional NES. Nuclear export of the GFP reporter was restored by the GR DBD, resulting in equilibration of the reporter between nuclei in the heterokaryon fusion (Figure 4b).

The GFP reporter used in the experiments described above contains the ligand binding domain of GR to direct Dex-dependent import. We used another GFP reporter, which lacked any GR sequence, to formally test for the sufficiency of the DBD export signal. The GFP reporter

used contains the SV40 large T antigen NLS to direct constitutive import, but it remains nuclear in the heterokaryon because it does not contain a nuclear export signal (Figure 4c, upper panels). Fusion of the GR DBD to the reporter resulted in nucleocytoplasmic shuttling (Figure 4c, lower panels). Thus, the GR DBD is sufficient to direct nuclear export of the GFP reporter.

We next transfected full-length nuclear receptors (GR, AR, and RAR) containing either a wt DBD or a mutant DBD (FF→AA) into donor cells, treated the cells with ligand, and fused them with acceptor cells labeled with the CellTracker dye. The wt forms of GR, AR, and RAR equilibrated between nuclei in the heterokaryon fusion (Figure 4d), indicating that export of these nuclear receptors occurs even in the presence of ligand. The DBD mutant forms (FF→AA) of GR and AR, however, failed to equilibrate between nuclei in the heterokaryon fusion. Thus, export of GR and AR from the donor nuclei is inhibited by changing only two amino acids within the DBD of each nuclear receptor. Surprisingly, the DBD mutant form of RAR still equilibrated between nuclei in the heterokaryon fusion (Figure 4d). Because the DBD of RAR is sufficient to specify nuclear export of the GFP reporter used in our analysis (Figure 2), we interpret this

Figure 2



as evidence that RAR export can occur by an alternative, DBD-independent transport pathway. Nuclear export of RXR in nerve cells can be facilitated by its binding partner NGFI-B, an orphan nuclear receptor with three leucine-rich NESs [22]. Nuclear export of the wild-type and mutant forms of RAR, however, still occurs in the presence of leptomycin B (data not shown). Certain nuclear receptors may, therefore, be exported from the nucleus by more than one transport pathway.

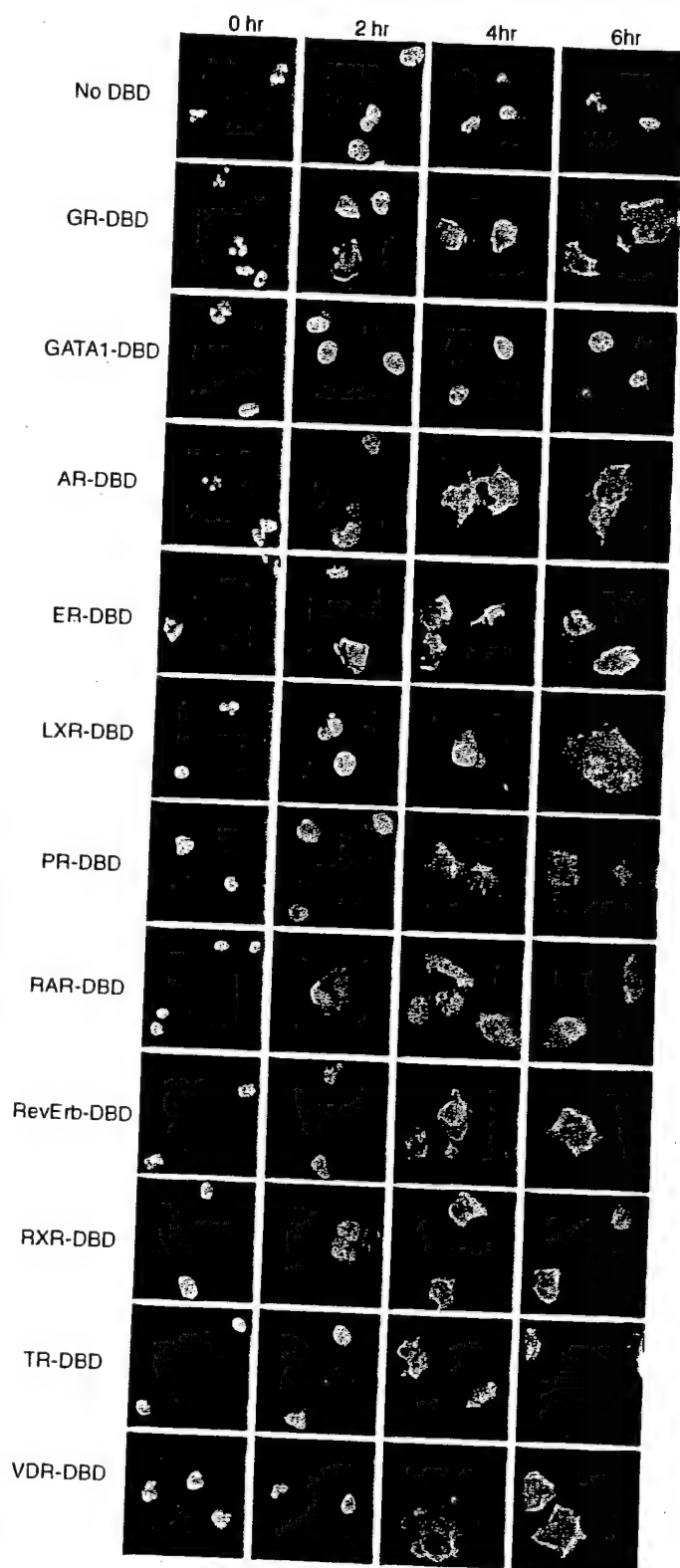
CRT binding to the GR DBD is required for nuclear export

Our results showing that the GR DBD functions as an export signal together with our previous finding that GR export is defective in *crt*^{-/-} cells suggested a molecular mechanism for the transport pathway [17]. This could involve CRT-dependent recognition of the GR DBD in the nucleus and translocation of the complex to the cytoplasm. We reasoned that if CRT binding to the DBD is an obligate step in GR export, then mutations within the DBD that inhibit export might also inhibit the interaction of GR with CRT. We tested this by using binding assays with recombinant CRT and glutathione-S-transferase (GST) fusions of the wt and mutant (FF→AA) forms of the GR DBD. CRT bound to the wt DBD but displayed only background binding to the GR DBD mutant protein (Figure 5a). Crm1 did not bind to the GR DBD, consistent with other data indicating that Crm1 is not the receptor for nuclear export of GR [16, 17].

The net redistribution of GR from the nucleus to the cytoplasm generally requires several hours in ligand-free media; however, the kinetics of export can be enhanced by microinjecting recombinant CRT into cells [17]. We used this approach to examine whether GR containing a wt or mutant DBD would undergo CRT-dependent nuclear export. Cos cells were transfected with GFP fused to full-length GR (wt or FF→AA mutant) and treated with ligand to induce nuclear import of GR. The cells were then injected with CRT, and the distribution of GR was recorded by fluorescence microscopy 30 min postinjection.

The DBD of GR functions as an NES. The GFP reporter engineered with the DBD of GR was transfected into Cos cells and assayed for nuclear export. Images of living cells were recorded by fluorescence microscopy at 0, 2, 4, and 6 hr following Dex withdrawal. The GFP reporter alone (no DBD) remains nuclear during the course of the experiment, while including the GR DBD (residues 418–486) in the GFP reporter confers export by 4 hr. Point mutations in the GR DBD (C424A or C463A) slightly reduced the level of export, evident at 4 hr. The 15 residue sequence (KVFFKRAVEGQHNYL; residues 442–456) that resides between the two zinc binding loops was sufficient for export of the GFP reporter. Alanine-scanning mutagenesis of residue pairs in the DBD revealed that the FF→AA mutation in the DNA recognition helix causes a major defect in nuclear export. The KR→AA, VE→AA, and YL→AA mutations have an intermediate effect on nuclear export, and the KV→AA, GQ→AA, and HN→AA mutations have no effect on nuclear export.

Figure 3



The DBDs of diverse nuclear receptors can all function as an NES. The DBDs from hormone, nonhormone, and orphan nuclear receptors were analyzed for nuclear export activity in vivo by using the GFP reporter. The GFP reporter alone (no DBD) remains nuclear during the course of the experiment. The DBD from the transcription

We observed that injection of cells with CRT caused the relocalization of wt GR from the nucleus to the cytoplasm (Figure 5b, upper panels). In contrast, CRT injection into cells expressing the GR DBD mutant (FF→AA) did not affect GR distribution (Figure 5b, middle panels). Crm1 injection did not cause wt GR redistribution to the cytoplasm. Thus, a functional export signal within the DBD is necessary for CRT-dependent translocation of GR from the nucleus to the cytoplasm. Recombinant CRT can also mediate nuclear export of GR in a permeabilized cell assay [17], and this can be inhibited by the addition of the DBD from VDR (Figure 5c). The ability of the DBD from VDR to act as a competitive inhibitor of GR export indicates that CRT recognizes similar molecular determinants in the DBDs of different nuclear receptors.

Excess DBD blocks GR export and increases transcription

Our finding that the VDR DBD can act as a competitive inhibitor of GR export in permeabilized cells led us to examine whether overexpression of the VDR DBD fused to BFP would compete with the GR export pathway in living cells. Because the DBD of VDR also contains an NLS [23], it undergoes export and import but is concentrated in the nucleus at steady state. Expression of BFP alone did not affect nuclear export mediated by the GR-DBD examined at 0 and 5 hr (Figure 6, upper panels). In contrast, expression of BFP-VDR DBD inhibited GR-DBD export and resulted in nuclear accumulation of GR-DBD (Figure 6, middle panels). This effect required a functional DBD in VDR since mutating the conserved pair of phenylalanines in the DBD reversed the inhibition (Figure 6, lower panels). Our data support the hypothesis that a common pathway is used for nuclear export of both steroid (GR) and nonsteroid (VDR) nuclear receptors.

Inhibiting DBD-dependent export in vivo restricts GR to the nucleus, thereby blocking the nucleocytoplasmic shuttling cycle. This allowed us to examine whether blocking nuclear export could augment the GR-dependent transcription by increasing its dwell time in the nucleus. We also considered the possibility that nucleocytoplasmic shuttling could be necessary for the transcriptional activity of GR because, for example, cytoplasmic chaperones are required for ligand binding. GR-dependent transcription can be measured in the presence of excess VDR DBD because VDR does not bind to a GRE [24]. The response elements for GR and VDR differ in sequence, direction, and spacing of the half-sites.

factor GATA1, which is similar in size to the nuclear receptors and contains two zinc binding loops, does not confer nuclear export to the GFP reporter. The DBDs from nine different nuclear receptors (AR, ER, LXR, PR, RAR, RevErb, RXR, TR, and VDR) confer nuclear export activity to the GFP reporter.

Figure 4

The DBD export signal is necessary for hormone receptor shuttling in vivo. **(a)** Heterokaryon shuttling assays were performed with Cos cells transfected with full-length GR fused to GFP (FITC) and NIH 3T3 cells labeled with the dye CellTracker CMTMR (Rhodamine). When coseeded on coverslips and fused by brief (30 s) incubation in polyethylene glycol (Roche; 50% vol:vol), the Cos and 3T3 cells fuse and fluoresce red. Nucleocytoplasmic shuttling (export and import) of the GFP reporter results in equilibration of green fluorescence between the donor Cos cell nuclei and the acceptor 3T3 cell nuclei within the heterokaryon. Acceptor cell nuclei (white arrowheads) are also distinguished by centromeric foci that stained brightly with DAPI. **(b)** The GR DBD restores shuttling behavior to the GFP reporter that contains a nonfunctional NES. **(c)** The GR DBD confers shuttling activity to a GFP reporter that contains the SV40 large T antigen NLS [38]. The GFP reporter contains the streptavidin gene and assembles into a ~160 kDa tetramer that is too large to escape the nucleus by diffusion. **(d)** The DBD export signal is necessary for nucleocytoplasmic shuttling in the context of full-length hormone receptors. Full-length wt or mutant (FF→AA) GR, AR, and RAR were tested for nucleocytoplasmic shuttling in the presence of 1 μ M Dex, 10 nM R1881 (synthetic androgen), or 1 μ M all-trans retinoic acid, respectively. Each wt receptor equilibrates between the nuclei of a heterokaryon. The FF→AA mutation inhibits GR and AR shuttling, whereas the FF→AA mutation has only a slight effect on RAR shuttling. The FF→AA mutation in the GR DBD abolishes DNA binding in vitro, suggesting the mutation does not generate a nuclear retention signal (data not shown).

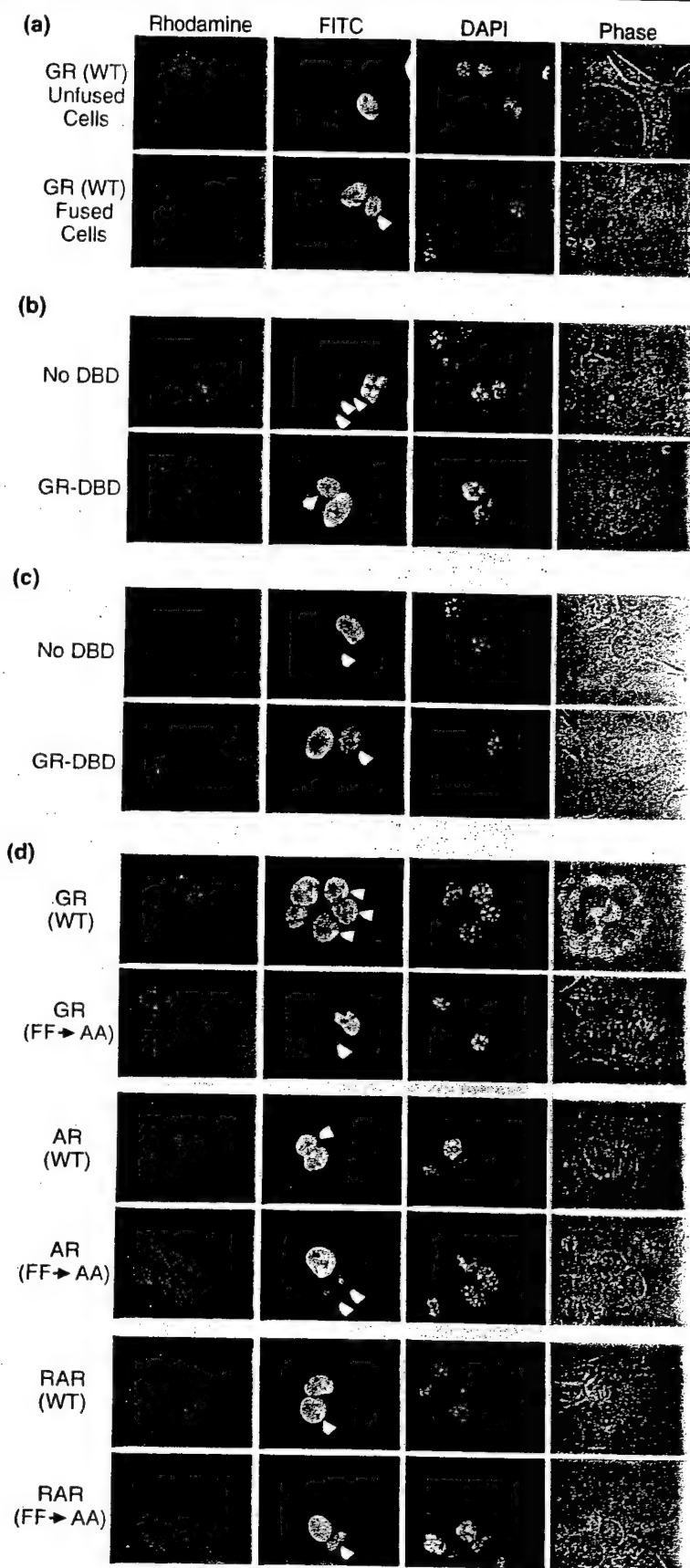
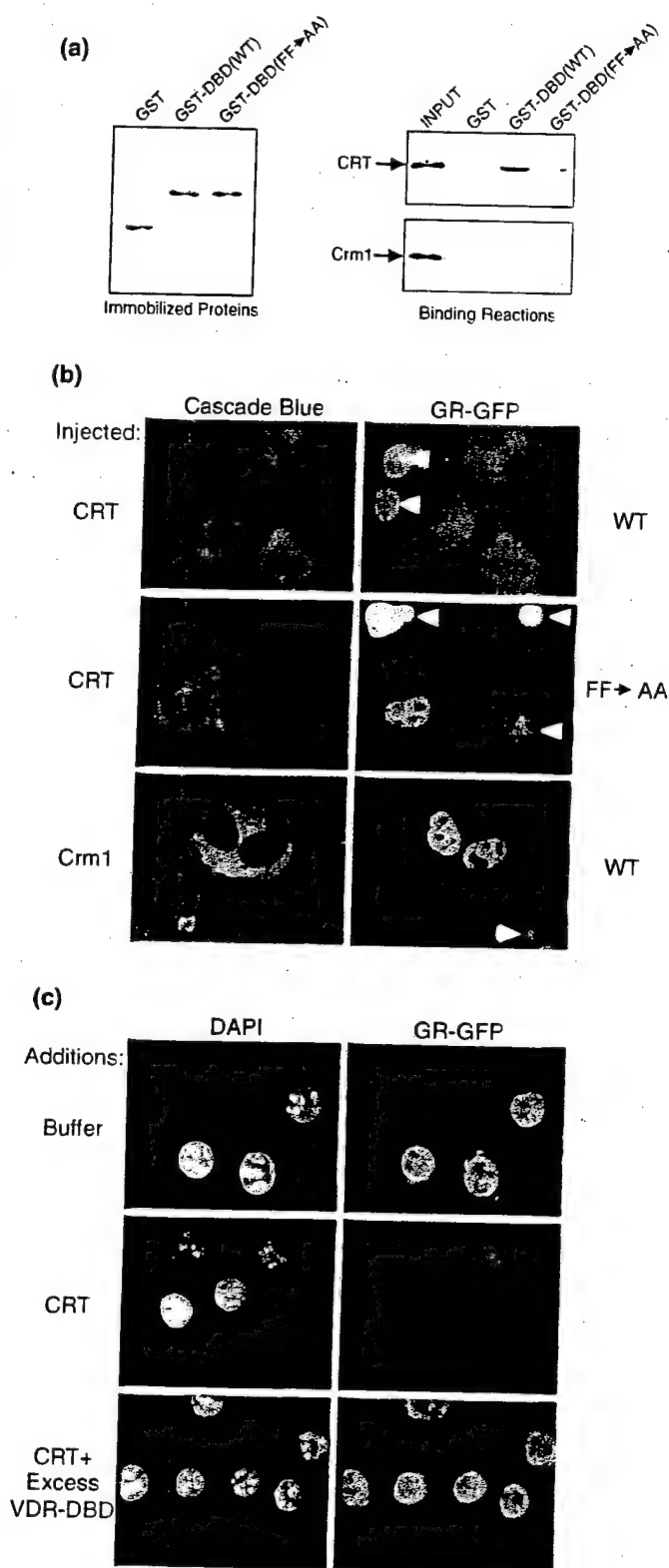


Figure 5

The DBD export signal is necessary for export mediated by CRT. **(a)** Direct binding of CRT to the GR DBD. GST fusion proteins containing the GR DBD (wt or FF→AA) were immobilized on glutathione-Sepharose beads and used for binding assays with recombinant CRT and Crm1. CRT binds to the wt DBD from GR but

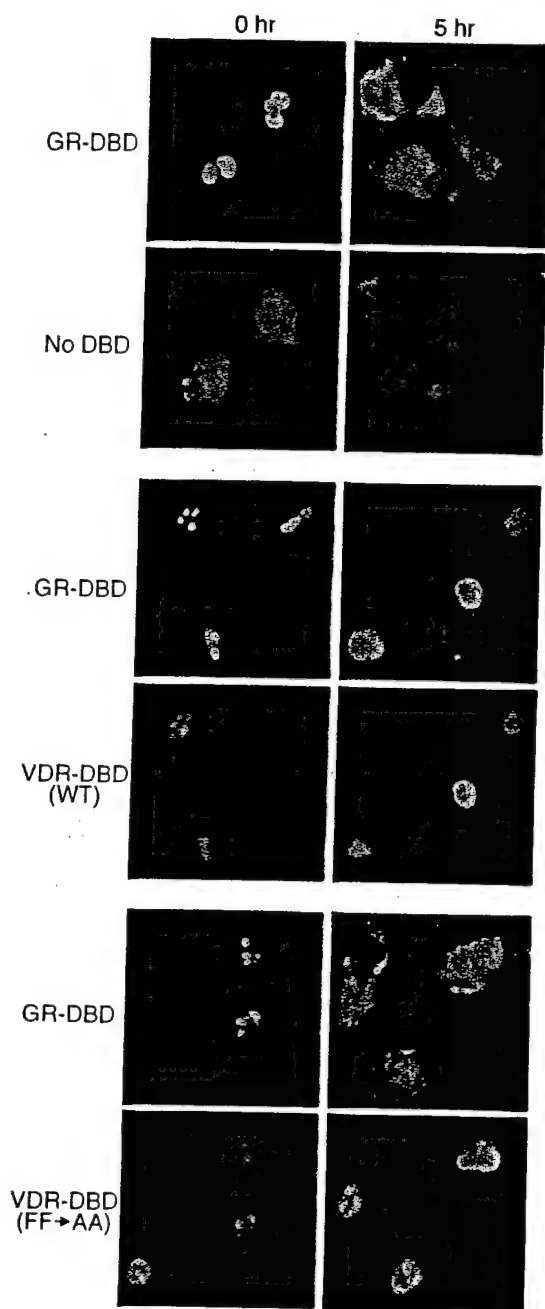
GR-dependent transactivation of a GRE-luciferase reporter was measured in the presence of cotransfected BFP or BFP-VDR DBD as a function of Dex concentration (Figure 7a). Expression of the BFP-VDR DBD increased GRE luciferase activity 2-fold relative to BFP. Thus, inhibiting GR export results in an increase in GR-dependent transcription. The effect was correlated with the amount of BFP-VDR DBD plasmid used for cotransfection (Figure 7b). We also found that a mutant form of the VDR DBD (FF→AA) that has reduced activity as a competitive inhibitor of GR export (Figure 6) increases the transcriptional activity of GR only slightly (Figure 7c). Our data indicate that nuclear export of GR is critical for proper regulation of its transcriptional activity, since blocking GR export results in an elevated response to ligand. Moreover, nuclear export is predicted to be important for regulating the cytoplasmic functions that are emerging for certain nuclear receptors.

Discussion

In the context of a living cell, GR undergoes rapid exchange between chromatin binding sites and the nucleoplasm [25]. Upon dissociating from chromatin, GR may receive input from signaling pathways that regulate its transcriptional activity, either in the form of posttranslational modifications or cofactor interactions [26]. This could occur in the nucleoplasm, or it could occur during the movement of GR through the cytoplasm during its shuttling cycle. The latter scenario would obviate the requirement for nuclear import of cytoplasmic enzymes, or cofactors, possibly to ensure spatial separation from the nuclear receptors. Because GR, AR, and RAR all shuttle in the presence of their respective ligand, nucleocytoplasmic shuttling is predicted to be a general property of nuclear

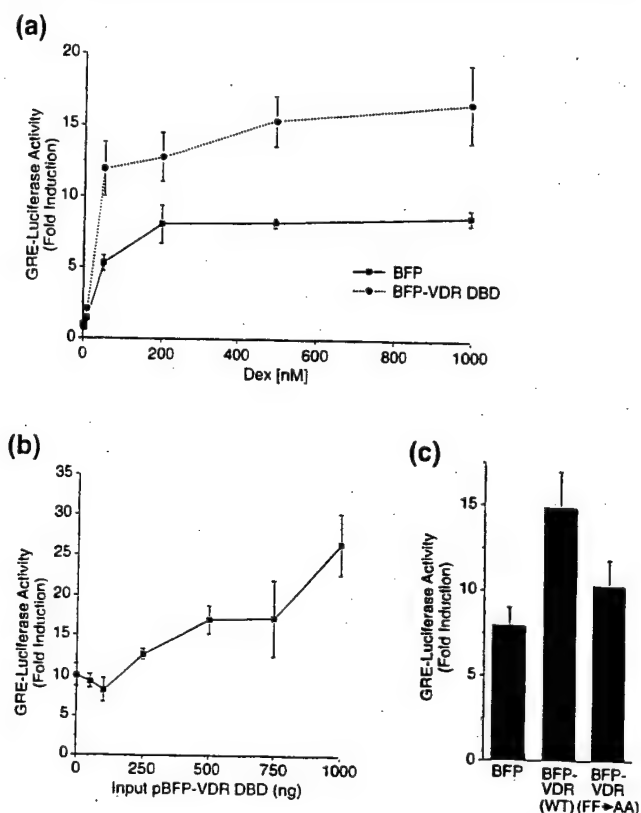
not to the export-defective mutant DBD (FF→AA) from GR. A preparation of recombinant Crm1 that binds the leucine-rich NES [39] does not bind to the DBD from GR. Shown are 5% of the total input proteins (CRT or Crm1). **(b)** CRT stimulates nuclear export of wt but not the export-defective mutant of GR in living cells. Cos cells transfected with GR (wt or FF→AA mutant) fused to GFP were treated with Dex to induce nuclear import. Following Dex withdrawal, the cells were microinjected with either His-tagged CRT or His-tagged Crm1 (1 mg/ml each), and the distribution of GR-GFP was examined after 30 min. A 70 kDa fluorescent dextran (Cascade Blue) was included to mark the injection site and to verify that the nuclear envelope remained intact during the experiment. CRT-dependent export of wt GR was observed in 30/30 cells injected, whereas CRT-dependent export of the mutant GR (FF→AA) was observed in only 2/21 cells injected (three experiments). GR did not undergo nuclear export in uninjected cells (white arrowheads) or Crm1-injected cells in this assay. The latter control is consistent with Crm1-independent export of GR [16, 17]. **(c)** Shared mechanism for nuclear export of GR and VDR. A cell line expressing GR-GFP [35] was permeabilized with digitonin and incubated with recombinant CRT (100 µg/ml) in the absence and presence of the DBD from VDR (120 µg/ml). CRT-dependent export of GR-GFP is blocked by the VDR DBD.

Figure 6



Competition for DBD-mediated export in vivo. The GFP reporter engineered with the DBD of GR was cotransfected with a plasmid encoding BFP alone (no DBD) or BFP fused to the DBD of VDR in Cos cells. Images were captured at 0 and 5 hr following Dex withdrawal. BFP alone did not alter import of the reporter alone (data not shown) or the import and export of the reporter containing the DBD of GR. The DBD of VDR (VDR-DBD [wt]) blocks GR DBD-mediated nuclear export. However, a mutant VDR DBD that has two critical phenylalanines replaced with alanines (VDR-DBD [FF→AA]) does not compete for GR DBD-mediated nuclear export.

Figure 7



Blocking GR export increases ligand-induced gene expression. **(a)** VDR-DBD expression increases GR-mediated gene expression over a wide range of Dex concentration. Endogenous GR activity was examined in NIH3T3 cells using a GRE-luciferase reporter. Cells were cotransfected in 6 well dishes with plasmids encoding a *Renilla*-luciferase reporter (30 ng), GRE-firefly luciferase (370 ng), and either BFP alone or BFP-VDR DBD (1000 ng), and then they were incubated overnight. Cells were lysed 6 hr following the addition of the indicated amount of Dex. **(b)** Increasing input pBFP-VDR DBD increases Dex-induced gene expression. Transfectants were incubated overnight and then treated with Dex (500 nM) for 6 hr prior to lysis. **(c)** Expression of a VDR DBD mutant that fails to compete for GR DBD-mediated nuclear export only slightly increases Dex-induced gene expression. Plasmids encoding either wt or FF→AA mutant versions of BFP-VDR DBD (500 ng each) were transfected and assayed as above. All luciferase assays were normalized for transfection efficiency using *Renilla*-luciferase expression. The values shown represent the fold induction by the addition of Dex and are the averages of triplicate wells plus or minus the standard deviation.

receptors. This would integrate cytoplasmic signaling events with regulation of nuclear transcription [27]. Alternatively, the function of DBD-dependent export may relate to cytoplasmic functions for nuclear receptors that may be transcription-independent [28–30].

Our finding that the DBD of nuclear receptors performs dual targeting functions in the cell is not without precedent. The DBD in Gal4 contains an NLS, and the DBD in Stat1 contains a leucine-rich NES that targets it for export by the Crm1 pathway [31, 32]. Thus, protein do-

mains that bind DNA provide suitable structures for presenting signals to the nuclear transport machinery. Nuclear transport receptor binding to a DBD-containing protein should, in addition, block the interaction of the protein with DNA. In the case of GR and probably other nuclear receptors, this may impart negative regulation on transcription even prior to nuclear export [18–20]. Nuclear export facilitated by DBDs and nuclear import facilitated by ligand-regulated NLSs illustrate how simple nuclear transport-based mechanisms are used to regulate the activity of a superfamily of transcriptional activators and influence gene expression in multiple biological pathways.

Materials and methods

Nuclear receptor cDNAs

The DBD from human GR was subcloned from the previously described plasmid pK7-GR-GFP [33]. The GenBank accession numbers corresponding to the other nuclear receptor superfamily members used for the DBD analysis are: rat AR, M23264; rat ER α , NM_012689; human LXR α , NM_005693; human PR, NM_000926; human RAR α , NM_000964; human RevErbA α , X72631; human RXR α , NM_002957; human TR β , X04707; and human VDR, NM_000376. Mutations were made using the QuickChange system (Stratagene).

Nuclear export assays

In vivo export assays

The reporter used to test DBD-mediated nuclear export has been described [17] and is derived from the plasmid pXM10 [34]. Cos7 cells were seeded onto coverslips and grown overnight prior to transfection of the reporter vectors using the transfection reagent Fugene 6 (Roche). All BFP-DBD competition experiments used plasmids derived from pEBFP-C (Clontech). The transfectants were grown overnight prior to addition of Dex (1 μ M) for 45–60 min. Cells were washed five times with serum-free and phenol red-free Dulbecco's modified eagle medium (DMEM) and incubated for the indicated times in phenol red-free DMEM containing 10 μ g/ml cyclohexamide and 10% charcoal stripped newborn calf or fetal bovine serum. Cells were fixed in formaldehyde (3.7%) and processed for fluorescence microscopy. Digital images were captured by a charge-coupled device camera (Hamamatsu ORCA) mounted on a Nikon Microphot-SA microscope, with Openlab (version 2.0.6) software. Figures were assembled with Adobe Photoshop (version 5.5) and Freehand (version 9). The examples shown are representative of 20–50 cells observed in two or more independent experiments.

In vitro export assays

A cell line expressing GR-GFP [35] was treated with 1 μ M Dex for 45 min. Cells were permeabilized with 0.005% digitonin for 5.5 min. Export reactions were performed at 30°C for 30 min in transport buffer (20 mM Hepes [pH 7.4], 110 mM potassium acetate, 2 mM magnesium acetate, and 1 mM EGTA) supplemented with an ATP-regeneration system, 2 mM dithiothreitol (DTT), and a protease inhibitor cocktail including aprotinin, leupeptin, and pepstatin (each at 1 μ g/ml). GFP images were captured with the same exposure times.

Heterokaryon analysis

The modified interspecies heterokaryon analysis was performed as follows. NIH3T3 cells were labeled in tissue culture dishes with 500 nM CellTracker dye, (5 (and 6)-((4-chloromethyl) benzoyl) amino) tetramethylrhodamine (CMTMR; Molecular Probes), according to the manufacturers instructions. Unincorporated dye was removed and cells were trypsinized and coseeded on glass coverslips with Cos7 cells that had been transfected with the indicated plasmids using the transfection reagent Fugene 6 (Roche). Equal numbers of each cell type were seeded for a total of 3×10^5 cells per 35 mm dish and grown overnight prior to fusion. The indicated ligands were added to the cells 45 min prior to

fusion, in order to induce nuclear accumulation of the reporter proteins. Cells were incubated at 37°C for 4 hr postfusion in the presence of the indicated nuclear receptor ligands and 10 μ g/ml cyclohexamide to block protein synthesis. Cells were then fixed and processed for fluorescence microscopy. AR was expressed with an N-terminal FLAG epitope and detected by indirect immunofluorescence using the monoclonal antibody M2 (Sigma) at a dilution of 1:2000. Goat anti-mouse fluorescein conjugated secondary antibody (Pierce) was used at a dilution of 1:100. GR and RAR were expressed as GFP fusions and detected in the FITC channel. The examples shown are representative of 10–25 heterokaryons from two or more independent experiments.

Microinjection analysis

Cos7 cells were transfected with the indicated vectors and grown overnight in 60 mM dishes; 1.2×10^5 cells per 35 mM dish were seeded onto gridded coverslips and grown overnight. Cells were treated with 1 μ M Dex for 45 min to induce nuclear import of the reporter proteins. Following Dex withdrawal, cells were microinjected with the indicated transport factors and a cascade blue injection marker (1 mg/ml; MW = 70 kDa) using femtotips mounted on a Micromanipulator and Transjector (Eppendorf). Cells were incubated 30 min at 37°C and then fixed and processed for fluorescence microscopy.

Recombinant proteins

Mouse CRT was subcloned in pQE-30 (Qiagen) for expression as a His-tagged protein in the TG1 *E. coli* strain. Cultures were grown in Luria Broth for 24 hr at 37°C without induction, and His-CRT was purified on TALON beads (Clontech), eluted with imidazole, and dialyzed into 50 mM Hepes (pH 7.4). The expression and purification of His-Crm1 has been described [36]. Recombinant transport factors were flash-frozen in single-use aliquots and stored at –80°C. The nuclear receptor DBDs were expressed in *E. coli* as GST fusions by using pGEX-2T and pGEX-4T vectors (Pharmacia). Cells were grown in Luria Broth, and protein expression was induced when OD₆₀₀ reached 0.5, with 1 mM IPTG. The cells were collected by centrifugation, resuspended in lysis buffer (25 mM Tris [pH 7.5] and 150 mM sodium chloride), and sonicated at 5°C until lysis was complete. The lysate was centrifuged at $15,000 \times g$ for 60 min, and the supernatant was loaded onto a glutathione-Sepharose column. The column was equilibrated and washed extensively with the lysis buffer, and GST-DBDs were eluted with the same buffer supplemented with 10 mM fresh glutathione. The GST-DBD proteins, in some cases, were cleaved with thrombin (Sigma) to generate the free DBDs. The GST and thrombin were removed using a strong cation exchange media SP-Sepharose (Pharmacia). The column was developed with 25 mM Tris buffer and a 150–500 mM sodium chloride gradient, with the GST and thrombin eluting at the beginning of the gradient and the free DBDs eluting at 300–350 mM sodium chloride.

Binding assays

His-CRT or His-Crm1 (each at 1 μ g/ml) proteins were incubated for 30 min at 4°C with the indicated GST proteins immobilized on glutathione-Sepharose beads. Binding reactions were carried out in 0.5X transport buffer supplemented with 10 mg/ml bovine serum albumin, 2 mM DTT, and 0.2% Tween-20. Beads were subsequently washed three times, and bound proteins were eluted with SDS-PAGE sample buffer and analyzed by Western blotting. CRT was detected using an anti-CRT rabbit polyclonal antibody (Stressgen), and Crm1 was detected using an anti-Crm1 rabbit polyclonal antibody (kindly provided by Ralph Kehlenbach, Scripps) [37].

Luciferase assays

Transcriptional reporter activity was measured by using the Dual-Luciferase Reporter Assay System (Promega) according to the manufacturer's directions. NIH3T3 cells were seeded at 2×10^5 per well of a 6 well dish and grown overnight prior to transfection. Transfections of the indicated plasmids were performed with the Cytofectene transfection reagent (Bio Rad). The Renilla-luciferase (R-Luc; Promega) and GRE-luciferase (generously provided by Gordon Hager, NIH) reporter vectors were used in all cases. The total input DNA was 1.4 μ g per well in

each experiment. Transfectants were grown overnight in phenol red-free DMEM containing 10% charcoal stripped fetal bovine serum prior to the indicated Dex treatments. Cells were washed with phosphate-buffered saline and lysed with 300 μ l passive lysis buffer (Promega). Luciferase activities were measured by using a Berthold LB 953 luminometer.

Acknowledgements

We thank our University of Virginia colleagues D. Allis, D. Burke, B. Pearson, L. Pemberton, and D. Wotton for reading the manuscript. We also thank G. Hager, J. Hanover, I. Macara, M. Weber, D. Wojchowski, and D. Wotton for their kind gifts of reagents, and M. Skerzinski and N. Mou for technical assistance. Financial support from the National Institutes of Health (GM58639-01 to B.M.P.) and the Department of Defense (DAMD 17-00-1-0048 to F.R.) is gratefully acknowledged.

References

- Evans RM: The steroid and thyroid hormone receptor superfamily. *Science* 1988, 240:889-895.
- Mangelsdorf DJ, Thummel C, Beato M, Herrlich P, Schütz G, Umesono K, et al.: The nuclear receptor superfamily: the second decade. *Cell* 1995, 83:835-839.
- McKenna NJ, Lanz RB, O'Malley BW: Nuclear receptor coregulators: cellular and molecular biology. *Endocrinol Rev* 1999, 20:321-344.
- Hager GL, Lim CS, Elbi C, Baumann CT: Trafficking of nuclear receptors in living cells. *J Steroid Biochem Mol Biol* 2000, 74:249-254.
- Picard D, Yamamoto KR: Two signals mediate hormone-dependent nuclear localization of the glucocorticoid receptor. *EMBO J* 1987, 6:3333-3340.
- Georget V, Lobaccaro JM, Terouanne B, Mangeat P, Nicolas JC, Sultan C: Trafficking of the androgen receptor in living cells with fused green fluorescent protein-androgen receptor. *Mol Cell Endocrinol* 1997, 129:17-26.
- Nakiely S, Dreyfuss G: Transport of proteins and RNAs in and out of the nucleus. *Cell* 1999, 99:677-690.
- Wente SR: Gatekeepers of the nucleus. *Science* 2000, 288:1374-1377.
- Tyagi RK, Lavrovsky Y, Ahn SC, Song CS, Chatterjee B, Roy AK: Dynamics of intracellular movement and nucleocytoplasmic recycling of the ligand-activated androgen receptor in living cells. *Mol Endocrinol* 2000, 14:1162-1174.
- Guiochon-Mantel A, Lescop P, Christin-Maitre S, Loosfelt H, Perrot-Appanat M, Milgrom E: Nucleocytoplasmic shuttling of the progesterone receptor. *EMBO J* 1991, 10:3851-3859.
- Madan AP, DeFranco DB: Bidirectional transport of glucocorticoid receptors across the nuclear envelope. *Proc Natl Acad Sci USA* 1993, 90:3588-3592.
- Baumann CT, Maruvada P, Hager GL, Yen PM: Nuclear cytoplasmic shuttling by thyroid hormone receptors. Multiple protein interactions are required for nuclear retention. *J Biol Chem* 2001, 276:11237-11245.
- Bunn CF, Neidig JA, Freidinger KE, Stankiewicz TA, Weaver BS, McGrew J, et al.: Nucleocytoplasmic shuttling of the thyroid hormone receptor α . *Mol Endocrinol* 2001, 15:512-533.
- Komeili A, O'Shea EK: Nuclear transport and transcription. *Curr Opin Cell Biol* 2000, 12:355-360.
- Tyagi RK, Amazit L, Lescop P, Milgrom E, Guiochon-Mantel A: Mechanisms of progesterone receptor export from nuclei: role of nuclear localization signal, nuclear export signal, and Ran guanosine triphosphate. *Mol Endocrinol* 1998, 12:1684-1695.
- Liu J, DeFranco DB: Protracted nuclear export of glucocorticoid receptor limits its turnover and does not require the exportin 1/CRM1-directed nuclear export pathway. *Mol Endocrinol* 2000, 14:40-51.
- Holaska JM, Black BE, Love DC, Hanover JA, Paschal BM: Calreticulin is a receptor for nuclear export. *J Cell Biol* 2001, 152:127-140.
- Burns K, Duggan B, Atkinson EA, Famulski KS, Nemer M, Bleackley RC, et al.: Modulation of gene expression by calreticulin binding to the glucocorticoid receptor. *Nature* 1994, 367:476-480.
- Dedhar S, Rennie PS, Shago M, Hagesteijn CY, Yang H, Filmus J, et al.: Inhibition of nuclear hormone receptor activity by calreticulin. *Nature* 1994, 367:480-483.
- Wheeler DG, Horsford J, Michalak M, White JH, Hendy GN: Calreticulin inhibits vitamin D3 signal transduction. *Nucleic Acids Res* 1995, 23:3268-3274.
- Omichinski JG, Clore GM, Schaad O, Felsenfeld G, Trainor C, Appella E, et al.: NMR structure of a specific DNA complex of Zn-containing DNA binding domain of GATA-1. *Science* 1993, 261:438-446.
- Katagiri Y, Takeda K, Yu ZX, Ferrans VJ, Ozato K, Guroff G: Modulation of retinoid signalling through NGF-induced nuclear export of NGFI-B. *Nat Cell Biol* 2000, 2:435-440.
- Hsieh JC, Shimizu Y, Minoshima S, Shimizu N, Haussler CA, Jurutka PW, et al.: Novel nuclear localization signal between the two DNA-binding zinc fingers in the human vitamin D receptor. *J Cell Biochem* 1998, 70:94-109.
- Freedman LP, Towers TL: DNA binding properties of the vitamin D₃ receptor zinc finger region. *Mol Endocrinol* 1991, 5:1815-1826.
- McNally JG, Muller WG, Walker D, Wolford R, Hager GL: The glucocorticoid receptor: rapid exchange with regulatory sites in living cells. *Science* 2000, 287:1262-1265.
- DeFranco DB, Qi M, Borror KC, Garabedian MJ, Brautigan DL: Protein phosphatase types 1 and/or 2A regulate nucleocytoplasmic shuttling of glucocorticoid receptors. *Mol Endocrinol* 1991, 5:1215-1228.
- Doucas V, Shi Y, Miyamoto S, West A, Verma I, Evans RM: Cytoplasmic catalytic subunit of protein kinase A mediates cross-repression by NF- κ B and the glucocorticoid receptor. *Proc Natl Acad Sci USA* 2000, 97:11893-11898.
- Migliaccio A, Castoria G, Di Domenico M, de Falco A, Bilancio A, Lombardi M, et al.: Steroid-induced androgen receptor-oestradial receptor β -SRC complex triggers prostate cancer cell proliferation. *EMBO J* 2000, 19:5406-5417.
- Simoncini T, Hafezi-Moghadam A, Brazil DP, Ley K, Chin WW, Liao JK: Interaction of oestrogen receptor with the regulatory subunit of phosphatidylinositol-3-OH kinase. *Nature* 2001, 407:538-541.
- Kousteni S, Bellido T, Plotkin LI, O'Brien CA, Bodenner DL, Han L, et al.: Nongenotropic, sex-nonspecific signaling through the estrogen or androgen receptors: dissociation from transcriptional activity. *Cell* 2001, 104:719-730.
- Silver PA, Keegan LP, Plashne M: Amino terminus of the yeast GAL4 gene product is sufficient for nuclear localization. *Proc Natl Acad Sci USA* 1984, 81:5951-5955.
- McBride KM, McDonald C, Reich NC: Nuclear export signal located within the DNA-binding domain of the STAT1 transcription factor. *EMBO J* 2000, 19:6196-6206.
- Carey KL, Richards SA, Lounsbury KM, Macara IG: Evidence using a green fluorescent protein-glucocorticoid receptor chimera that the Ran/TC4 GTPase mediates an essential function independent of nuclear protein import. *J Cell Biol* 1996, 133:985-996.
- Love DC, Sweitzer TD, Hanover JA: Reconstitution of HIV-1 Rev nuclear export-independent requirements for nuclear import and export. *Proc Natl Acad Sci USA* 1998, 95:10608-10613.
- Walker D, Htun H, Hager GL: Using inducible vectors to study intracellular trafficking of GFP-tagged steroid/nuclear receptors in living cells. *Methods* 1999, 19:386-393.
- Englmeier L, Olivo JC, Mattaj JW: Receptor-mediated substrate translocation through the nuclear pore complex without nucleotide triphosphate hydrolysis. *Curr Biol* 1999, 9:30-41.
- Kehlenbach RH, Dickmanns A, Gerace L: Nucleocytoplasmic shuttling factors including Ran and CRM1 mediate nuclear export of NFAT in vitro. *J Cell Biol* 1998, 141:863-874.
- Black BE, Lévesque L, Holaska JM, Wood TC, Paschal BM: Identification of an NTF2-related factor that binds Ran-GTP and regulates nuclear protein export. *Mol Cell Biol* 1999, 19:8616-8624.
- Black BE, Holaska JM, Lévesque L, Ossareh-Nazari B, Gwizdek C, Dargemont C, et al.: NXT1 is necessary for the terminal step of Crm1-mediated nuclear export. *J Cell Biol* 2001, 152:141-155.

Ca²⁺-Dependent Nuclear Export Mediated by Calreticulin

James M. Holaska,^{1,2†} Ben E. Black,^{1,3‡} Fraydoon Rastinejad,^{3,4}
and Bryce M. Paschal^{1,3*}

Center for Cell Signaling¹ and Departments of Microbiology,² Biochemistry and Molecular Genetics,³
and Pharmacology,⁴ University of Virginia, Charlottesville, Virginia 22908

Received 22 January 2002/Returned for modification 6 March 2002/Accepted 23 May 2002

We have characterized a pathway for nuclear export of the glucocorticoid receptor (GR) in mammalian cells. This pathway involves the Ca²⁺-binding protein calreticulin (CRT), which directly contacts the DNA binding domain (DBD) of GR and facilitates its delivery from the nucleus to the cytoplasm. In the present study, we investigated the role of Ca²⁺ in CRT-dependent export of GR. We found that removal of Ca²⁺ from CRT inhibits its capacity to stimulate the nuclear export of GR in digitonin-permeabilized cells and that the inhibition is due to the failure of Ca²⁺-free CRT to bind the DBD. These effects are reversible, since DBD binding and nuclear export can be restored by Ca²⁺ addition. Depletion of intracellular Ca²⁺ inhibits GR export in intact cells under conditions that do not inhibit other nuclear transport pathways, suggesting that there is a Ca²⁺ requirement for GR export *in vivo*. We also found that the Ran GTPase is not required for GR export. These data show that the nuclear export pathway used by steroid hormone receptors such as GR is distinct from the Crm1 pathway. We suggest that signaling events that increase Ca²⁺ could positively regulate CRT and inhibit GR function through nuclear export.

The nuclear transport machinery integrates a variety of nuclear and cytoplasmic activities by mediating the translocation of housekeeping and regulatory proteins and RNAs. Translocation of these macromolecules generally requires a *cis*-acting transport signal, recognition of the signal by a receptor, and movement of the signal-receptor complex through the nuclear pore complex (NPC) (40, 45). In the case of nuclear export, most proteins rely on a hydrophobic nuclear export signal (NES) and its recognition by the receptor Crm1 (1, 10, 11, 39, 44). NES binding to Crm1 is stabilized by the presence of RanGTP, and the resulting trimeric complex of Crm1, NES, and RanGTP undergoes translocation through the nuclear pore (14, 28). Other proteins are important cofactors for this export pathway, including RanGAP, RanBP1, NXT1, and RanBP3 (1, 4, 22, 24).

A number of proteins that lack a hydrophobic NES are known to undergo nuclear export, and current evidence indicates that three distinct mechanisms can account for nuclear export of these proteins. First, an NES-containing adapter could be used to bridge the interaction between the protein and Crm1 (21). Second, the protein could use a different signal for nuclear export and undergo Crm1-independent export (3). Third, the protein could interact directly with nucleoporins in the NPC and undergo receptor-independent nuclear export (46). An advantage of these mechanisms is that they provide the potential for additional levels of regulation for protein sorting between the nucleus and cytoplasm.

The glucocorticoid receptor (GR) is an example of a protein that undergoes export from the nucleus even though it lacks a hydrophobic NES. Moreover, GR export is insensitive to the Crm1 inhibitor leptomycin B, which seems to rule out the use of NES adapters and Crm1 as the major receptor for this pathway (18, 25). The signal that specifies nuclear export of GR maps to the 67-amino-acid DNA binding domain (DBD), which is both sufficient to mediate the export of green fluorescent protein (GFP) reporter proteins and necessary for export of GR (3). Mutations that disrupt DBD structure, whether in the context of an isolated DBD or in full-length GR, also reduce its export activity. The most severe mutations that reduce DBD-dependent nuclear export are two phenylalanine-to-alanine mutations in the DNA recognition helix (3). The structural conservation of the DBD in the nuclear receptor superfamily suggests that the DBD could be widely used as an export signal. Support for this hypothesis was obtained by showing that the DBDs from steroid, nonsteroid, and orphan nuclear receptors can function as export signals when fused to a GFP reporter protein (3).

Nuclear export mediated by the DBD of GR involves a Ca²⁺-binding protein named calreticulin (CRT), which was first described as a protein in the lumen of the endoplasmic reticulum (ER) (29). The original link between these proteins came with the finding that a peptide sequence, KLGFFKR, which is recognized by CRT, is related to the peptide sequence KVFFKR, which is found in the DNA recognition helix of GR (33). CRT binds to GR and blocks its interaction with DNA in gel shift experiments, and overexpression of CRT inhibits GR-dependent transcription in cells (6). Similar results were obtained when the interactions between the androgen, retinoic acid, and vitamin D receptors and CRT were examined (8). The initial interpretation of these results was that a pool of CRT outside of the lumen of the ER acts as a negative regulator of transcription. The technical difficulty of showing that CRT is out-

* Corresponding author. Mailing address: Box 800577 Hospital West, Health Sciences System, University of Virginia, Charlottesville, VA 22908. Phone: (434) 243-6521. Fax: (434) 924-1236. E-mail: paschal@virginia.edu.

† Present address: Department of Cell Biology, Johns Hopkins University School of Medicine, Baltimore, MD 21205.

‡ Present address: Ludwig Institute for Cancer Research, University of California, San Diego, CA 92093.

side the ER, however, gave way to the view that CRT is restricted to the ER lumen and that the effects of CRT on gene expression are indirect (23).

Our laboratory purified CRT from HeLa cell cytosol in a search for novel export factors (18). We used a permeabilized cell assay that measures the nuclear export of protein kinase inhibitor (PKI), a protein that contains a hydrophobic NES (19). CRT can bind directly to the NES in PKI, which contains the peptide sequence LALKLAGLDIN. In binding experiments the interaction of CRT with PKI is stabilized in the presence of RanGTP, and in permeabilized cells CRT-dependent export of PKI is enhanced by RanGTP (18). The ability of CRT to act as an export factor for PKI and its prior link with steroid receptor function led us to test whether CRT can function as an export factor for GR. We found that recombinant CRT can stimulate GR export and that the GR export deficiency in *crt*^{-/-} cells can be rescued with CRT (18). These observations support the view that CRT functions as an export factor for GR.

In the present study we characterized the CRT-dependent nuclear export of GR, with particular emphasis on how this pathway could be regulated. Because CRT is a Ca²⁺ binding protein, we have examined how removing Ca²⁺, either by chelation or by deletion of Ca²⁺ binding domains, affects CRT binding to the GR DBD and CRT-dependent nuclear export of GR. We show that Ca²⁺ binding to CRT is necessary for direct binding to the DBD and for nuclear export of GR in permeabilized cells. This Ca²⁺ requirement involves the C-terminal domain of CRT, which contains multiple low-affinity, high-capacity binding sites for Ca²⁺ (2). Removal of the C-terminal domain renders CRT insensitive to Ca²⁺ chelation, suggesting that this domain performs a regulatory function that is linked to Ca²⁺ binding. While the Ca²⁺-loaded CRT is active for GR export and Ca²⁺-free CRT is inactive for GR export, the opposite is the case for NES export in permeabilized cells. Thus, Ca²⁺-loaded CRT is inactive for Rev export and Ca²⁺-free CRT is active for Rev export. The Ca²⁺-loaded and Ca²⁺-free forms of CRT were shown to have different sensitivities to proteases (7), indicating that CRT adopts different protein conformations. Our data show that these Ca²⁺-dependent conformations of CRT are correlated with the ability to recognize different protein substrates. Ca²⁺ depletion in vivo results in the inhibition of GR export, consistent with a Ca²⁺ requirement for the translocation of GR from the nucleus to the cytoplasm. Our finding that CRT requires Ca²⁺ for binding and nuclear export of GR suggests a potential mechanism for regulating this pathway.

MATERIALS AND METHODS

Plasmids and recombinant proteins. Standard methods were used for the expression and purification of glutathione *S*-transferase (GST)- and His-tagged proteins, all of which were stored at -80°C as single-use aliquots. The plasmid encoding the GST fusion with CRT was constructed in pGEX4T3, using the open reading frame of mouse CRT lacking the N-terminal 17-amino-acid signal sequence. GST-CRT was expressed in DH5α bacteria as described previously (18). Full-length and deletion mutants of mouse CRT were cloned into pQE30, and the His-tagged proteins were expressed in TG1 bacteria (3). The wild-type (WT) and NES mutant forms of PKI (L41A, L44A) (44) were expressed in BL21(DE3) bacteria and purified without fusion tags as described previously (19). The plasmid encoding a hydrophobic NES was generated by cloning the DNA sequence that encodes residues 35 to 49 of human PKI into pGEX4T3. Likewise, the plasmid encoding a nuclear receptor DBD was generated by cloning

the DNA sequence that encodes residues 413 to 509 of human GR (3). The GST-NES and GST-DBD proteins immobilized on glutathione beads were either used directly for binding experiments or eluted and used in microtiter plate binding assays. For certain competition experiments, WT and mutant (MUT) forms of the GR DBD (FF to AA) were expressed as GST fusion proteins, cleaved from GST using thrombin, and further purified by ion-exchange chromatography (3). Plasmids encoding His-tagged Ran (WT, Q69L, and T24N; a gift of D. Görlich) and His-tagged Crm1 (a gift of L. Gerace) were used to express proteins in TG1 bacteria, which were purified on Talon resin (Clontech).

Binding assays. The three formats used for the solid-phase binding assays were microtiter wells, biosensor cuvettes, and Sepharose beads. The microtiter well assay was performed as described previously (4). Briefly, purified target proteins were immobilized in high-binding 96-well plates (Costar no. 3590) overnight at 4°C in 1× transport buffer (30). Unbound protein was removed, and the plates were blocked overnight with bovine serum albumin (30 mg/ml). Binding assays (with 100-μl mixtures) were performed in triplicate, using radiolabeled Ran and CRT or Crm1, and the level of binding was measured by scintillation counting as described previously (4). The biosensor assay was performed as described previously (18). Briefly, biotinylated NES peptide was immobilized in streptavidin-coated cuvettes (Fisons) for 15 min at room temperature. The cuvettes were washed with PBS and used for binding assays with the proteins indicated in the legend to Fig. 3. A detailed description of the Fisons biosensor, which measures the change in refractive index that occurs on protein-ligand binding and dissociation, has been published (34). The Sepharose bead binding assays, using either glutathione beads and GST proteins or Talon beads and His-tagged proteins, were carried out by standard methods. Briefly, proteins were immobilized on the beads and blocked overnight with bovine serum albumin (30 mg/ml), and the assays (with 100-μl mixtures) were performed using the proteins indicated in the legends. The bound fractions were examined by immunoblotting using antibodies to CRT or Crm1 and enhanced chemiluminescence.

Ca²⁺ removal from CRT. Ca²⁺ was removed from CRT by a published procedure that involves treatment with EGTA (43). Recombinant CRT (0.5 mg/ml in PBS) was incubated for 10 min at 30°C in the presence of 10 mM EGTA, and the sample was then transferred to ice. Ca²⁺ was rebound to CRT by supplementing half of the EGTA-treated sample with excess CaCl₂ (final Ca²⁺ concentration, 20 mM). The EGTA- and Ca²⁺-treated samples were used at a dilution of at least 1:10 in nuclear export and binding assays, such that the maximum concentration of EGTA in the assays was ~1 mM.

GR export assays. Nuclear export of GR in permeabilized cells was performed essentially as described previously (18), except that a stable cell line expressing GR-GFP (a gift of G. Hager) was used instead of transiently transfected cells. The cell line (3676 cells) (27) expresses GR-GFP under the control of a tetracycline-regulated promoter. The cells were grown on glass coverslips for 16 h in the absence of tetracycline to allow GR-GFP expression, and nuclear import of GR-GFP was induced in vivo by dexamethasone (Dex; 1 μM) addition to the media. The cells were permeabilized with digitonin (0.005%) for 5 min and used for export assays in vitro with the combinations of transport factors indicated in the legends. At the end of the 20-min export reaction, the samples were washed, fixed, stained with 4',6-diamidino-2-phenylindole (DAPI), and mounted on glass slides. Using a Nikon Microphot SA microscope (60× objective, numerical aperture N.A. = 1.40) and a Hamamatsu C-4742-95 charge-coupled device camera, ~50 nuclei from each coverslip were selected using the DAPI channel and DAPI and GFP images were captured. The digital images were acquired using Openlab 2.06 on a Macintosh G3 computer (OS 9.0), and figures were assembled using Adobe Photoshop 5.5 and Freehand 9.0. Mixtures for reactions that measured export and import in the same nuclei contained, in addition to CRT or Crm1, the fluorescent protein allophycocyanin coupled with NLS peptide (APC-NLS) and recombinant import factors (importins and NTF2).

Hydrophobic NES export assays. The assay for nuclear export of Rev in permeabilized cells has been described previously (RGG2.2 cells) (18, 26). The fluorescent reporter in this cell line (denoted Rev-GFP) also contains the ligand binding domain of GR, which confers Dex-inducible import in vivo. Digitonin permeabilization, nuclear export, and analysis using fluorescence microscopy were performed as described above for GR-GFP. All export assay mixtures contained Ran, NXT1, and RanBP1. In experiments designed to test the role of Ran in CRT-dependent export, the T24N and Q69L mutant forms of Ran were preloaded with unlabeled GDP and GTP, respectively, and unincorporated nucleotide was removed on a desalting column.

Ca²⁺ depletion in living cells. Nuclear export of GR was assayed under conditions of Ca²⁺ depletion in the 3676 cells by measuring the net redistribution from the nucleus to the cytoplasm. Cells expressing GR-GFP were treated with Dex for 1 h to induce nuclear import and subsequently transferred to phenol red-free media containing ionomycin (Ion; 1 μM) or thapsigargin (TG; 1 μM) in

the presence of 1,2-bis(*O*-aminophenoxy)ethane-*N,N,N',N'*-tetraacetic acid-acetoxymethyl ester (BAPTA-AM; 10 μ M). Cells were also treated with dimethylsulfoxide (DMSO; 0.1%) as a control since the Ion and TG were prepared as 1,000 \times stocks in DMSO. At 0-, 3-, and 6-h time points, the coverslips were fixed in formaldehyde (3.7%) and mounted using Vectashield. The ratio of nuclear to cytoplasmic GR-GFP fluorescence was measured using Openlab software in at least 50 cells per condition. Similar methods were used to assay the effect of Ca^{2+} depletion on Rev-GFP export using the RGG2.2 cells.

RESULTS

Assembly of CRT complexes in vitro. In digitonin-permeabilized cells, CRT can stimulate the nuclear export of proteins such as PKI that contain a hydrophobic NES, in a reaction that is dependent on Ran (18). In addition, CRT can stimulate the nuclear export of steroid hormone receptors that lack a hydrophobic NES. The export signal for CRT-dependent export of steroid hormone receptors is contained within the DBD of these proteins (3). The lack of apparent structural similarity between the hydrophobic NES and the DBD led us to characterize how CRT can recognize distinct export signals.

Because Ran is a stoichiometric component of export complexes that contain Crm1 and NES proteins, we first examined whether Ran might also function as a component of export complexes that contain CRT. Previously, we have shown that Ran assembles into a complex containing NES and CRT (18). In the present study, we tested whether Ran can assemble into a complex containing the DBD of GR (amino acids 413 to 509) and CRT. WT PKI, NES MUT PKI, and GST-DBD were immobilized in microtiter wells and incubated with recombinant CRT or Crm1 (5 μ g each) in the presence of radiolabeled RanGTP (2×10^4 cpm). RanGTP assembled into a complex with CRT or Crm1 in the presence of WT PKI. The reaction is specific since a functional NES in PKI is required for complex assembly. In contrast to these results obtained with the NES-containing protein PKI, RanGTP did not coassemble into a complex with CRT or Crm1 in the presence of the DBD from GR (Fig. 1A). Thus, CRT binding to the DBD is qualitatively different from CRT binding to the hydrophobic NES, since only the latter involves RanGTP as a stoichiometric component.

We carried out binding reactions with the DBD immobilized on glutathione beads and confirmed that CRT binds directly to the DBD and that binding is neither enhanced nor prevented by RanGTP (Fig. 1B). Under the reaction conditions, Crm1 binding to the hydrophobic NES was stimulated by the presence of RanGTP (lane 6). We did not observe Crm1 binding to the DBD in the absence or presence of RanGTP, consistent with our data that Crm1 is not the receptor for proteins that use the DBD as an export signal (18). Our data demonstrate that CRT can assemble into two types of export complexes in vitro: a CRT-NES-RanGTP complex and a CRT-DBD complex.

Ran-dependent and Ran-independent export by CRT. The results of our binding assays suggested that CRT-mediated export might occur by both Ran-independent and Ran-dependent mechanisms. That is, the data suggested that nuclear export of hydrophobic NES-containing proteins could be Ran dependent and nuclear export of DBD-containing proteins could be Ran independent. We tested this hypothesis by manipulating the composition and concentration of recombinant export factors in permeabilized cell assays, using GFP fusions of Rev and GR as the export substrates to assay NES- and

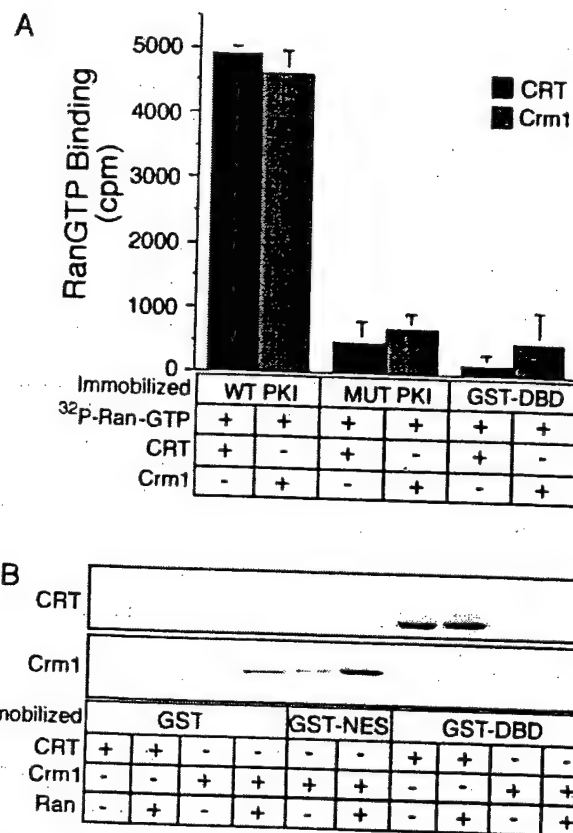


FIG. 1. Formation of export complexes involving CRT and Crm1. (A) The incorporation of RanGTP into complexes containing CRT and Crm1 was assayed using Ran preloaded with [γ - 32 P] GTP. Target proteins were immobilized in microtiter wells (500 ng/well), and CRT or Crm1 (5 μ g each) was added to each well together with 2×10^4 cpm of radiolabeled RanGTP. Following incubation for 1 h at room temperature, the wells were washed four times and the bound fractions were released and assayed by scintillation counting. (B) RanGTP is not a cofactor for CRT binding to the DBD. Target proteins (1 μ g each) were immobilized on glutathione beads, and CRT or Crm1 (500 ng each) was added to each sample in the absence or presence of Ran (1 μ g) preloaded with cold GTP. The samples were mixed end over end for 2 h at room temperature, washed three times, eluted, and analyzed by immunoblotting with antibodies to CRT and Crm1. These data show that, like Crm1, NES recognition by CRT involves RanGTP. In contrast, DBD recognition by CRT does not involve RanGTP.

DBD-dependent export, respectively. Both GFP export substrates contain the hormone binding domain of GR, which directs efficient Dex-dependent nuclear import in vivo (31). Following a digitonin permeabilization step, nuclear export of the GFP reporters can be stimulated by the addition of soluble transport factors (26).

We tested for the role of Ran in CRT-dependent NES export by using Rev, which contains a hydrophobic NES (LP-PLERLTL) (10). We used a concentration of CRT that was determined to be subsaturating with respect to Rev-GFP export. In the presence of 0.2 μ M CRT, WT Ran preloaded with GTP stimulated Rev-GFP export (Fig. 2A). In contrast, the Ran mutant T24N, which mimics the GDP-bound form of Ran, was inactive for CRT-dependent export. The Ran mutant Q69L, which mimics the GTP-bound form of Ran, showed little effect on export mediated by CRT, which is different from

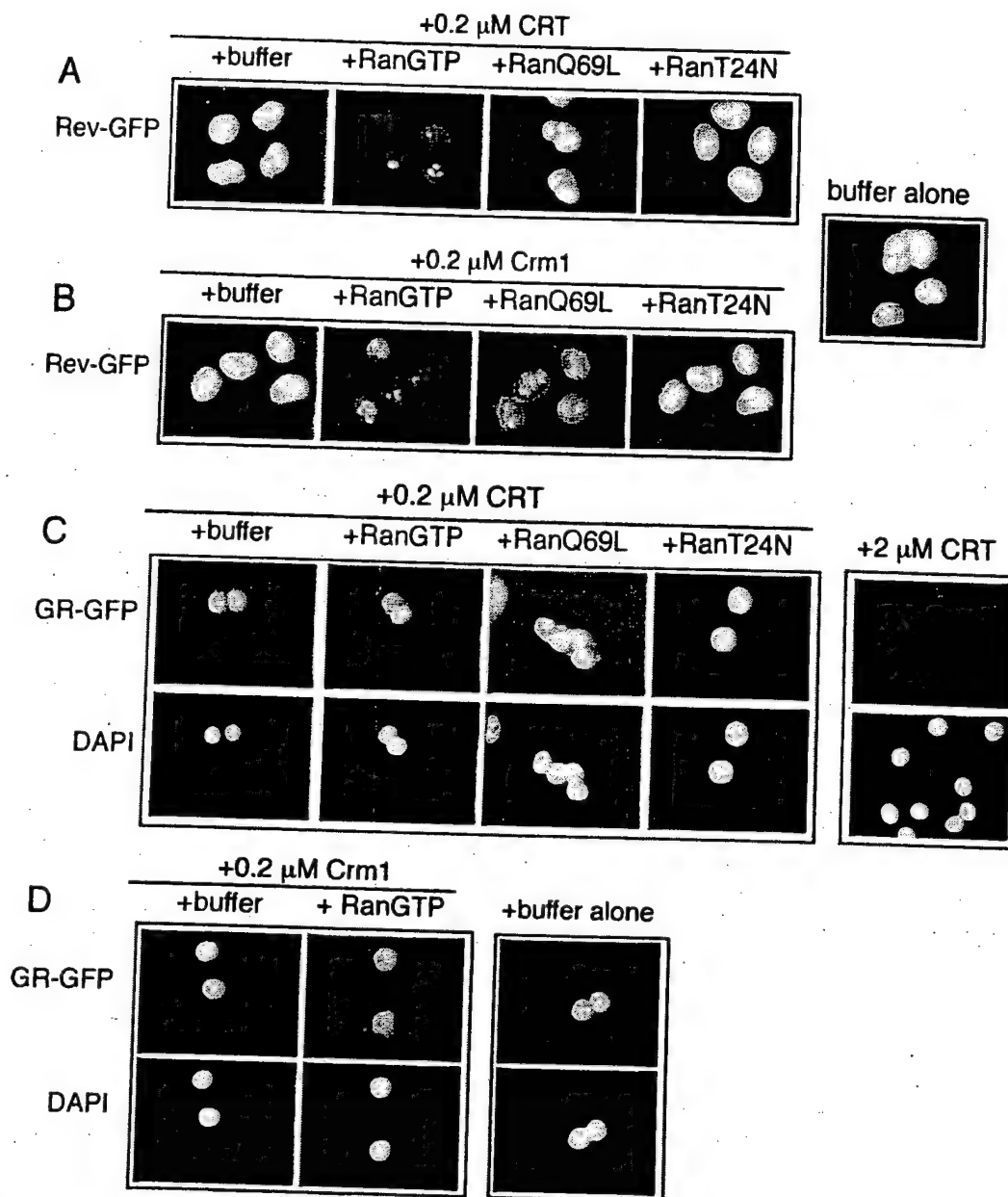


FIG. 2. Ran is a cofactor for NES-dependent export but not for DBD-dependent export. Nuclear export was assayed by supplementing digitonin-permeabilized cell assay mixtures with CRT (0.2 or 2.0 μM), Crm1 (0.2 μM), and different forms of Ran (1.9 μM each). NES-dependent export was assayed using a cell line that expresses a GFP fusion with Rev (RGG2.2) (26), and DBD-dependent export was assayed using a cell line that expresses a GFP fusion with GR (3676) (27). The Rev-GFP fusion also contains the ligand binding domain of GR, which imparts ligand-dependent nuclear import of the reporter protein. Prior to digitonin permeabilization, both cell lines were treated with Dex (1 μM) to induce nuclear import of the GFP reporters. (A and B) RanGTP stimulates Rev-GFP export in the presence of CRT or Crm1. (C and D) In contrast, neither WT nor MUT forms of Ran stimulate GR-GFP export in the presence of CRT or Crm1.

previous results obtained using another RanGTP mutant (G19V) and a fluorescent conjugate of PKI as the export substrate (18). The reason for this discrepancy is unclear, but it could relate to subtle differences in the structure and activity of these mutant proteins or to the fact that different NES proteins were used in the two assays, or both. Crm1 in these assays (Fig. 2B) supports robust export of Rev-GFP in the presence of WT Ran preloaded with GTP. In the presence of the Ran mutant Q69L, a moderate level of export was observed, while the Ran

mutant T24N failed to support Crm1-dependent export. Thus, Ran stimulates both CRT- and Crm1-dependent export in this system, and maximal export activity of either protein is observed only in the presence of WT Ran.

GR-GFP export was assayed at the same concentration of CRT (0.2 μM) that, in the presence of RanGTP, promotes efficient export of Rev GFP. We determined that the addition of subsaturating CRT together with Ran does not support nuclear export of GR. We also found that the addition of Crm1

and RanGTP at concentrations (0.2 and 1.9 μ M, respectively) that promote efficient Rev export fails to support GR export. These transport data correlate with our *in vitro* binding data, since CRT-dependent binding and export of an NES-containing protein is dependent on RanGTP. In contrast, CRT-dependent binding and export of the DBD appears to be independent of Ran. In the context of permeabilized cell assays, CRT can substitute for Crm1 in the NES pathway; however, Crm1 cannot substitute for CRT in the DBD pathway.

Overlapping export substrate binding sites on CRT. We considered two models to account for the ability of CRT to bind and mediate the nuclear export of two substrates with apparently unrelated export signals. In the first model, CRT could contain two distinct substrate binding sites, with only one of the two sites regulated by RanGTP. In the second model, CRT could contain a single substrate-binding site that accommodates both types of substrate and could use RanGTP to regulate the binding of only one of the two types of substrate. We reasoned that if CRT uses a single substrate binding site (or a single type of binding site), then CRT binding to the DBD should be inhibited in the presence of excess NES. To address this issue, we assayed CRT binding to an immobilized DBD in the absence and presence of WT and NES mutant forms of PKI. CRT binding to the DBD was reduced by the presence of WT PKI but not by the NES mutant form of PKI (Fig. 3A). Our data are consistent with a single type of substrate binding site on CRT, although we cannot rule out the possibility that CRT contains a second substrate binding site that is inhibited by an allosteric mechanism.

We also tested whether CRT contains a single type of substrate binding site by assaying nuclear export in permeabilized cells. Nuclear export of GR-GFP was tested in the absence and presence of WT and NES mutant forms of PKI. Inclusion of excess WT PKI (12 μ M) in the reaction mixture inhibited the nuclear export of GR, whereas inclusion of the NES mutant form of PKI at the same concentration had no effect (Fig. 3B). GR export mediated by CRT was blocked by excess GR DBD (4.5 μ M), consistent with previous data showing that the DBD functions as the signal for nuclear export of GR (3, 18).

The assays described above (Fig. 3A and B) were designed to measure the effect of excess NES on CRT binding to, and export of, the DBD. We performed analogous protein binding and nuclear export experiments that, instead, measured the effect of excess DBD on the interaction between CRT and the NES (Fig. 3C). In the biosensor assay, CRT binding to the NES (green tracing) or Crm1 binding to the NES (purple tracing) were both observed, but only in the presence of Ran GTP. CRT binding to the NES was reduced markedly by the presence of a WT DBD (light blue tracing), but this interaction was unaffected by the presence of a MUT DBD (dark blue tracing). The ability of the DBD to compete with NES for binding to CRT provides evidence that a single type of binding site is used for both substrates.

The effect of excess DBD on CRT-dependent export of NES substrate was tested in permeabilized cells by using Rev-GFP as a reporter. CRT-dependent export of Rev-GFP was inhibited by excess DBD and, as expected, by excess WT PKI (Fig. 3D). Addition of excess WT PKI resulted in inhibition of Crm1-dependent export of Rev-GFP, while addition of excess DBD had no effect on Rev-GFP export (data not shown). In

summary, our results demonstrate that (i) CRT can bind to and mediate the nuclear export of a protein that contains either a hydrophobic NES or a steroid hormone receptor DBD, (ii) CRT-dependent binding and export of a protein containing the hydrophobic NES is dependent on Ran, (iii) CRT-dependent binding and export of a protein containing an appropriate DBD is not dependent on Ran, and (iv) CRT uses a similar substrate binding site for proteins that contain either a hydrophobic NES or an appropriate DBD.

Ca²⁺ is critical for CRT export activity. CRT was originally discovered as a Ca²⁺ binding protein (29), and many of its functions in the ER have been proposed to be linked to its ability to bind Ca²⁺ (20). To determine if Ca²⁺ influences the nuclear export activity of CRT, we used an established method to release Ca²⁺ from recombinant CRT (43) and tested the protein in binding and transport assays. EGTA-induced Ca²⁺ release from CRT resulted in the loss of CRT binding to the DBD. Binding to the DBD was, however, restored by the addition of excess Ca²⁺ (Fig. 4A). Ca²⁺ removal from CRT caused a corresponding reduction in its capacity to promote nuclear export of GR in permeabilized cells, and the export activity was restored by the addition of excess Ca²⁺ (Fig. 4B). Unexpectedly, the capacity of CRT to mediate nuclear export of the NES substrate Rev-GFP was unaffected by EGTA, and the addition of excess Ca²⁺ to this assay actually inhibited Rev-GFP export (Fig. 4C). The effect of Ca²⁺ on Rev-GFP export appears to be linked to CRT since these treatments did not affect Crm1-dependent export of Rev-GFP (Fig. 4D). These data suggest that the Ca²⁺-bound state of CRT determines whether it binds to DBD- or NES-containing proteins and that these interactions are mutually exclusive under the conditions used in our assays.

We considered it formally possible that addition of EGTA to digitonin-permeabilized cells could block GR export by inhibiting NPC function. Ca²⁺ depletion in cells has been reported to inhibit the nuclear import of an NLS reporter protein (15), and there is structural evidence that depletion of Ca²⁺ from the lumen of the nuclear envelope can alter NPC structure (41). It was also possible that Ca²⁺-free CRT might accumulate at the NPC and block transit through the nuclear pore. We addressed this issue in a permeabilized cell assay that reconstitutes both nuclear import and export (Fig. 5A), reasoning that nuclear import would provide a relevant readout of NPC activity that is independent of nuclear export. Import in these assays was reconstituted by the addition of α - and β -importin, Ran, and NTF2 and was monitored by the nuclear accumulation of allophycocyanin conjugated with the simian virus 40 large T-antigen NLS (APC-NLS). EGTA effectively blocked GR export without affecting APC-NLS import (Fig. 5B). Moreover, excess Ca²⁺ blocked CRT-dependent export of Rev-GFP without affecting APC-NLS import. This effect was specific to CRT since Crm1-dependent export of Rev-GFP was unaffected by excess Ca²⁺ (Fig. 5C). Our data are consistent with Ca²⁺-mediated regulation of the activity of CRT and not with the inactivation of NPC function. We note that our standard assay buffer contains 1 mM EGTA. Because this condition is permissive for CRT-dependent export, removal of Ca²⁺ from CRT may require the higher concentration of EGTA (10 mM) or pretreatment of purified CRT with EGTA at 30°C, or both.

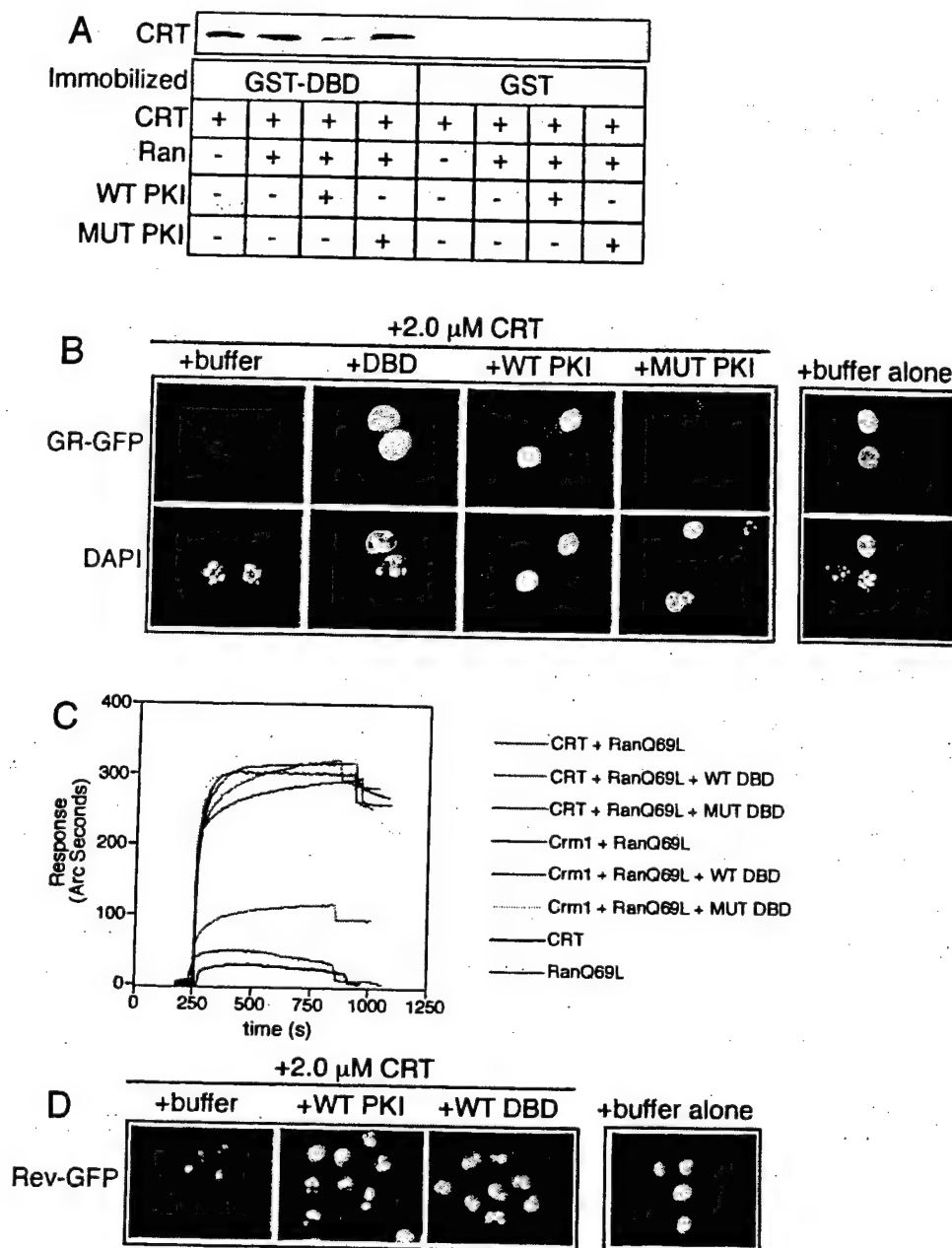


FIG. 3. The DBD and hydrophobic NES use a common or overlapping binding site on CRT. (A) Binding assay with GST-DBD or GST (2 μ g each) immobilized on glutathione beads and CRT (500 ng), RanGTP (2 μ g), and WT or MUT PKI (2 μ g) added in solution. The bound fractions were analyzed by immunoblotting for CRT. Including WT PKI in the reaction reduced the level of CRT bound to the DBD, indicating that these proteins bind to similar sites on CRT. This competition was not observed when RanGTP was omitted from the assay (data not shown), consistent with Ran acting as a cofactor for NES binding but not for DBD binding. (B) Nuclear export of GR-GFP was assayed in permeabilized cells using CRT (2.0 μ M) in the presence of buffer, excess DBD (4.5 μ M), or PKI (12 μ M WT or MUT). (C) Competitive binding interactions between NES, DBD, and CRT measured in a biosensor assay. NES peptide was immobilized on the cuvette surface through a biotin-neutravidin linkage and was used to measure the Ran-dependent binding of CRT in the absence and presence of DBD in the solution. The proteins used in the assay were CRT (1.1 μ M), Crm1 (1.1 μ M), RanQ69L (1.9 μ M), and WT and MUT DBD from GR (9.1 μ M each). CRT binds efficiently to NES peptide in the presence of Ran (green tracing), and this can be competed with the WT DBD (light blue tracing) but not with the transport-defective MUT DBD that contains the FF-to-AA mutations (dark blue tracing). Crm1 binding to the NES is unaffected by the presence of excess DBD (fuchsia tracing). (D) The DBD competes with NES in the CRT-dependent export pathway. The cell line expressing Rev-GFP was used to assay export in the presence of CRT (1.1 μ M), WT PKI (12 μ M), and WT DBD (9.1 μ M) as indicated.

The P-domain and C-terminal domain of CRT Impart Ca^{2+} regulation. As diagrammed in Fig. 6A, the domain structure of CRT includes an acidic C-terminal domain that contains multiple low-affinity, high-capacity Ca^{2+} binding sites ($K_D \approx 2$

mM; >25 mol/mol) and a proline-rich P-domain that contains high-affinity, low-capacity Ca^{2+} binding sites ($K_D \approx 1$ μ M) (2). In light of our data showing that Ca^{2+} can regulate CRT-dependent export of GR, we examined whether the C-terminal

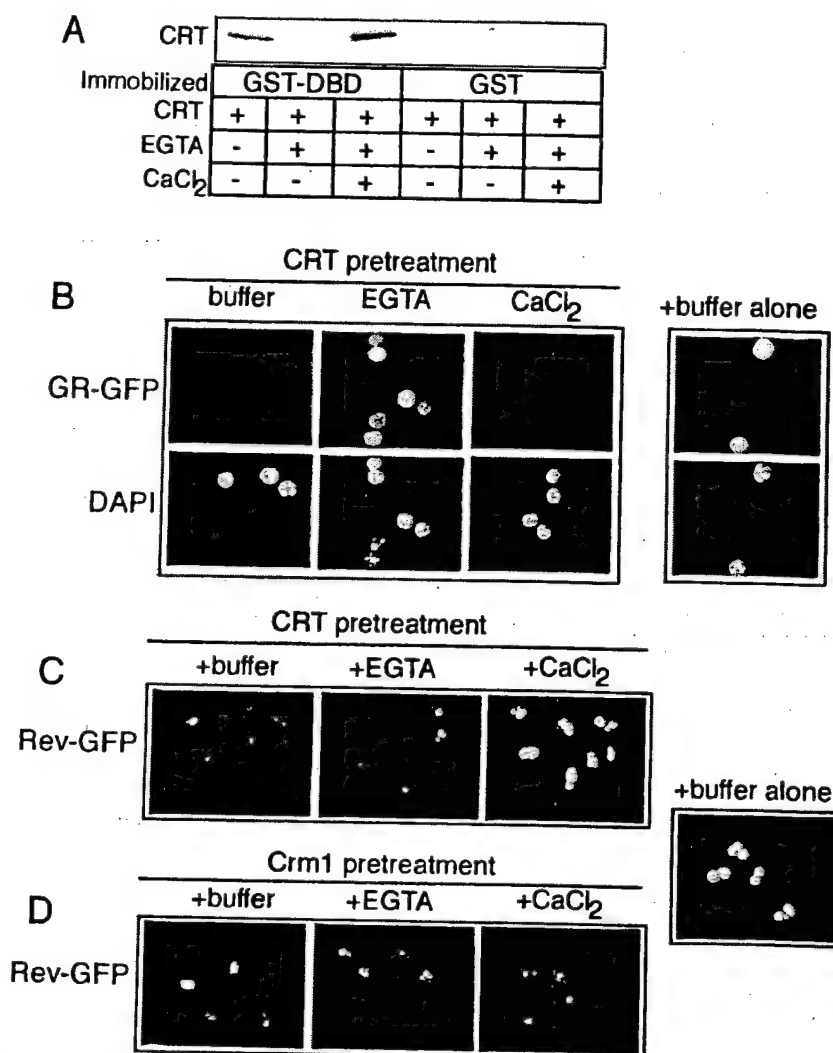


FIG. 4. Ca^{2+} binding to CRT is necessary for nuclear export of GR. (A) Binding assay performed with GST-DBD or GST (2.5 μg each) immobilized on glutathione beads and CRT (500 ng). The amount of CRT bound in each reaction fraction was examined by immunoblotting for CRT. The CRT used in the binding assay was untreated, pretreated with 10 mM EGTA, or pretreated with 10 mM EGTA and 20 mM CaCl_2 . Ca^{2+} removal from CRT inhibits binding to the DBD, and this can be reversed by addition of Ca^{2+} . (B and C) Ca^{2+} is required for CRT-dependent NES export; however, Ca^{2+} inhibits CRT-dependent NES export. (D) The presence of excess EGTA and Ca^{2+} in the permeabilized-cell assay mixture does not affect the export mediated by Crm1. CRT and Crm1 were used at a final concentration of 1.1 μM each in the export assays. The pretreatment of CRT and Crm1 with EGTA is described in Materials and Methods.

domain is required for CRT activity in our assays. CRT mutants lacking a portion of the C-terminal domain (retaining residues 1 to 350) or the entire C-terminal domain (retaining residues 1 to 273) were still functional for nuclear export of Rev-GFP, and the activities of these mutants was blocked by excess Ca^{2+} (Fig. 6B to D). From these data we infer that the Ca^{2+} -dependent inhibition of hydrophobic NES export by CRT can be ascribed to the high-affinity low-capacity Ca^{2+} binding site in the P-domain.

The deletion mutants were also examined for the Ca^{2+} dependence of DBD binding and GR export. We found that the deletion mutants still bound to the DBD in the presence of Ca^{2+} and that the mutant (residues 1 to 273) lacking the entire C-terminal domain was able to bind to the DBD in the presence of EGTA, albeit to a lesser extent than was the full-length CRT (Fig. 6E). This suggests that in the absence of Ca^{2+} , the

C-terminal domain normally exerts a negative regulation on the substrate binding activity of CRT. Removal of the entire C-terminal domain (residues 1 to 273) also resulted in loss of the EGTA-dependent inhibition of GR export that is observed with both the full-length and partial C-terminal domain deletion mutant (Fig. 6F to H). These data indicate that the low-affinity, high-capacity Ca^{2+} binding sites in the C-terminal domain of CRT are not required for nuclear export of hydrophobic NES or DBD-containing proteins but that they do contribute a regulatory function. The Ca^{2+} binding sites in the C-terminal domain are important for the EGTA-sensitive GR export, and the Ca^{2+} binding site in the P-domain appears to be sufficient to confer Ca^{2+} -induced inhibition of NES export.

GR-GFP Export is Sensitive to Ca^{2+} Depletion. Our results showing that GR undergoes CRT- and Ca^{2+} -sensitive export in permeabilized cells prompted us to examine whether this

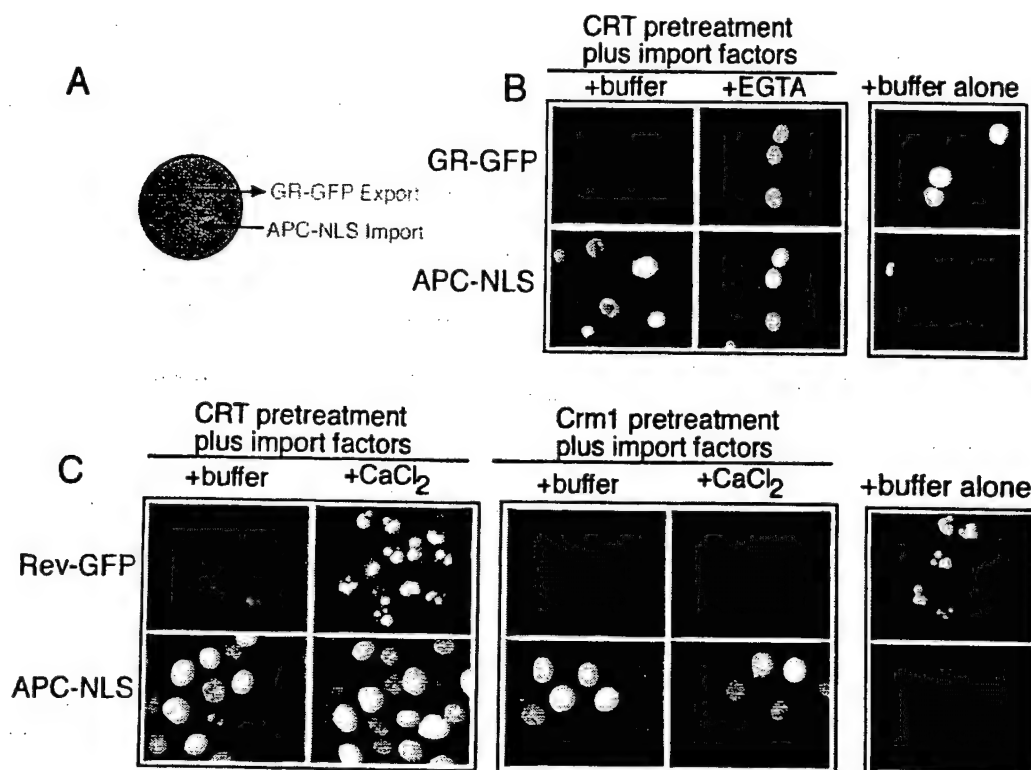


FIG. 5. Ca^{2+} chelation with EGTA inhibits CRT-dependent export without affecting nuclear import in permeabilized cells. (A) Diagram illustrating the assay for nuclear import (APC-NLS) and export (GR-GFP) in the same cells. (B) EGTA blocks CRT-dependent export of GR-GFP without affecting the nuclear import of APC-NLS in the presence of β -importin, Rch1, Ran, NTF2, NXT1, and RanBP1 (50 $\mu\text{g}/\text{ml}$ each). (C) Excess Ca^{2+} blocks CRT-dependent export of Rev-GFP without affecting the nuclear import of APC-NLS.

pathway is operational in living cells. The 3676 cell line (27), which stably expresses GR-GFP, was treated with Dex to induce import and then transferred to Dex-free medium that contained reagents known to deplete luminal and cytosolic Ca^{2+} . The effect of Ca^{2+} depletion on nuclear export was examined by fluorescence microscopy after 6 h and quantitated by measuring the nuclear/cytoplasmic fluorescence ratio of GR-GFP. The conditions included treatment with the Ca^{2+} ionophore Ion (1 μM) or the ER Ca^{2+} pump inhibitor TG (1 μM). The membrane-permeable form of BAPTA-AM (10 μM) was included with Ion and TG to chelate Ca^{2+} that was released. We found that Ion or TG administered in the presence of BAPTA-AM were both effective at blocking the nuclear export of GR-GFP (Fig. 7A). During the export phase of the experiment, the nuclear/cytoplasmic fluorescence in the control cells showed a significant reduction from 11.9 ± 2.1 to 1.5 ± 1.5 (Fig. 7B). In contrast, the nuclear/cytoplasmic fluorescence in the Ion- and TG-treated cells showed only a slight reduction, to 9.9 ± 1.2 and 10.5 ± 0.9 , respectively.

It is unlikely that Ion, TG, and BAPTA-AM cause a global disruption of NPC structure because NES-dependent export of Rev-GFP continues under Ca^{2+} depletion conditions in vivo (Fig. 7C) as well as in vitro (26). The transport of other cargos is unaffected by Ca^{2+} depletion in vivo, including Crm1-dependent nuclear export of mitogen-activated protein kinase-activated protein kinase 2 (42) and importin/karyopherin-dependent nuclear import of Rev-GFP (B. Black, unpublished observations). Our finding that nuclear export of GR in per-

meabilized cells is sensitive to the Ca^{2+} -bound state of the CRT used in the assays suggests that depletion of Ca^{2+} in vivo blocks the CRT-dependent export of GR in the cell.

DISCUSSION

Our study has revealed that Ca^{2+} and RanGTP can regulate the nuclear export activity of CRT. Ca^{2+} binding to CRT is necessary for its interaction with the DBD of GR in solid-phase binding assays and for nuclear export of GR in digitonin-permeabilized cell assays. These interactions appear to be independent of Ran, since Ran is not required for CRT binding to the DBD. Ran does not stimulate GR export when CRT is rate-limiting in the assay, and GTPase-deficient mutants of Ran do not block GR export. Under conditions where the low-affinity Ca^{2+} binding sites of CRT are saturated with Ca^{2+} , CRT does not support the nuclear export of a hydrophobic NES substrate. The export capacity for a hydrophobic NES substrate can be restored by EGTA-mediated removal of Ca^{2+} from CRT. Under these conditions of low Ca^{2+} , RanGTP acts as a stimulatory factor of CRT in a mechanism that involves the assembly of CRT, NES, and RanGTP into a complex (18). Collectively, our data suggest that Ca^{2+} binding determines whether CRT interacts with DBD containing cargo or with NES-containing cargo, and only the latter involves Ran.

The characterization of CRT over the past several years has revealed that it can associate with structurally distinct substrates (20). Studies of the chaperone-like functions of CRT

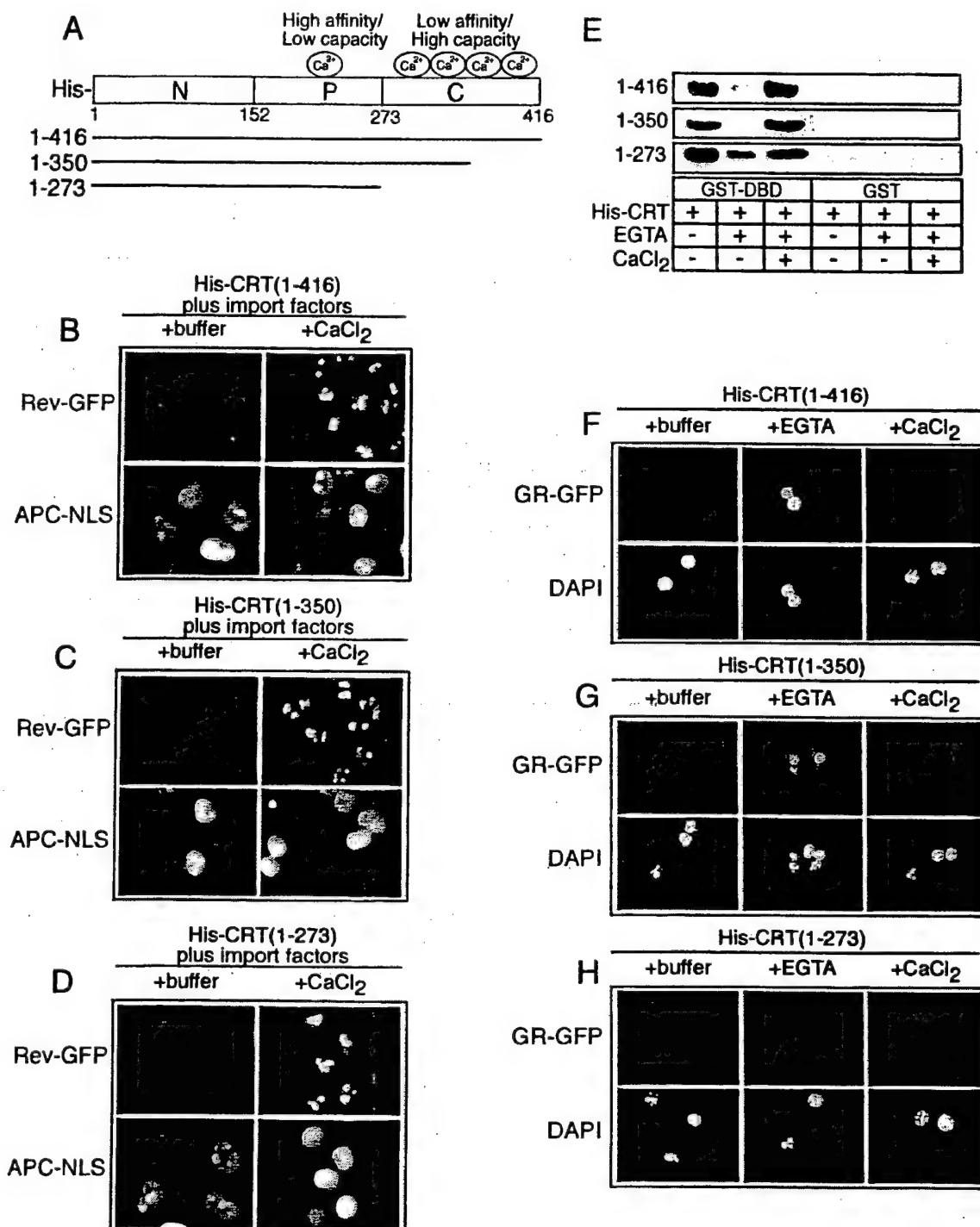


FIG. 6. The low-affinity Ca^{2+} binding sites in the C-terminal domain of CRT are not essential for nuclear export activity. (A) Diagram of the CRT structure and sites of Ca^{2+} binding. (B to D) Export assays performed with CRT proteins containing deletions in the low-affinity Ca^{2+} binding C-terminal domain. CRT lacking the entire C-terminal domain retains its Ca^{2+} -dependent inhibition of NES export, indicating that this is probably due to the high-affinity, low-capacity Ca^{2+} binding site. (E) EGTA-sensitive binding of CRT to the DBD is partially lost on removal of the C-terminal domain (residues 1 to 273). (F to H) Removal of the entire C-terminal domain (residues 1 to 273) from CRT abrogates the EGTA-sensitive export of GR. Although the C-terminal domain of CRT is not required for export, it is necessary for Ca^{2+} regulation of GR export.

proposed to occur in the ER lumen have addressed the in vitro interaction of CRT with oligosaccharides, both free in solution and as a structural component of glycoproteins. CRT is capable of binding directly to high-mannose-containing oligosac-

charides, and CRT can partially suppress the aggregation of certain glycosylated proteins exposed to elevated temperatures (35). It can also suppress the thermal aggregation of nonglycosylated proteins (35). These data have been taken as evi-

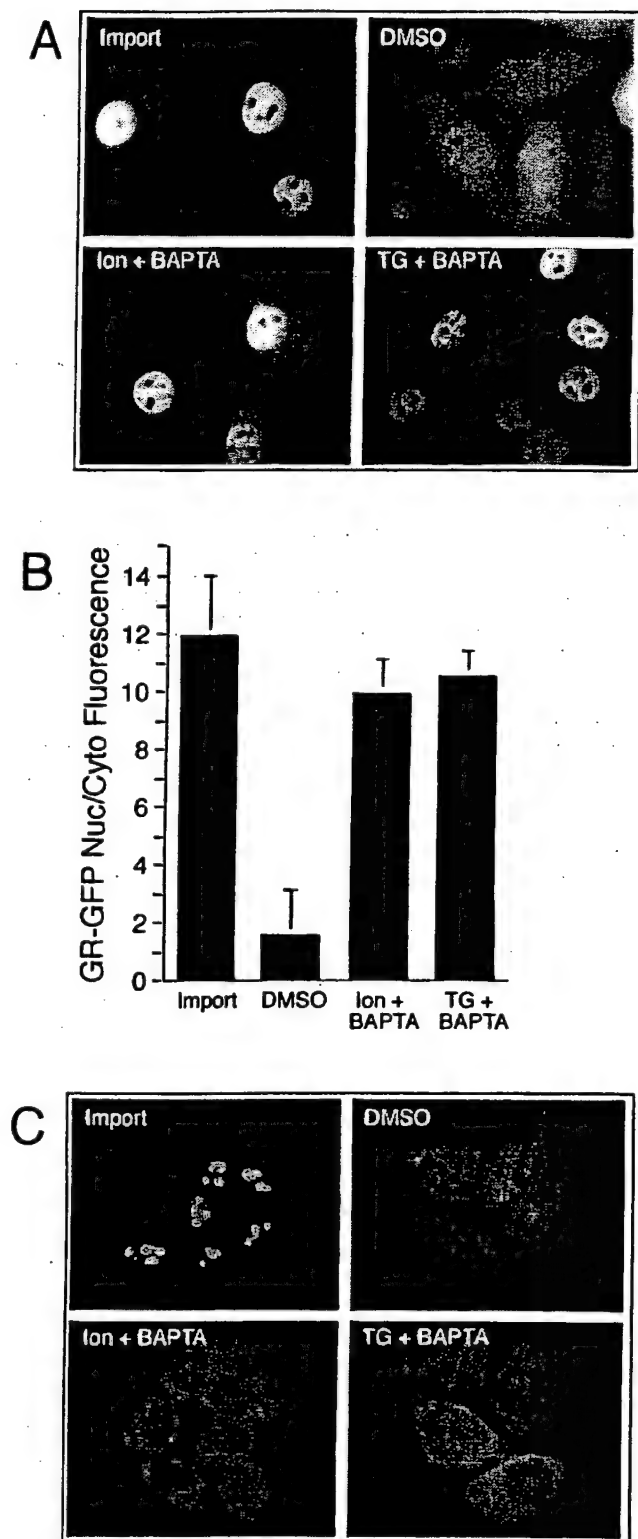


FIG. 7. Ca^{2+} depletion in vivo inhibits the nuclear export of GR. (A) Representative fields of cells expressing GR-GFP after induction of nuclear import with Dex (Import). Following Dex removal, the cells were treated for 5 h with vehicle (DMSO), Ion and BAPTA-AM, or TG and BAPTA-AM, and the GR-GFP distribution was recorded in living cells. (B) Measurements of the nuclear/cytoplasmic (Nuc/Cyto) ratios of GR-GFP fluorescence in cells incubated under conditions that deplete Ca^{2+} . Depletion of luminal stores of Ca^{2+} with Ion and

dence that in the ER, CRT may use both its lectin and peptide binding properties to stabilize protein-folding intermediates. The view that CRT participates in the folding of glycoproteins in the ER is logical, given the sequence relatedness (34% identity; expectation value, $<10^{-50}$) and functional similarities to the ER chaperone calnexin. Calnexin is a key component of a quality control pathway that monitors the folding state of glycoproteins in the ER. The current view is that calnexin and CRT interact transiently with protein-folding intermediates, effectively retaining them in the ER until a native conformation is attained (17).

Studies of the functions of CRT that occur outside the ER have yielded an even more diverse collection of substrates (20). These include the cytoplasmic domain of α -integrins (33), steroid hormone receptors (6), NES-containing proteins (18), and a stem-loop structure from rubella virus RNA (38). Some of these substrates contain a binding site for CRT that can be recognized at the sequence level, while other substrates seem structurally distinct. The site within α -integrin recognized by CRT is the sequence KXGFFKR, which is similar to the sequence KVFFKR within the DNA recognition helix of GR and other nuclear receptors. The NESs in PKI (LALKLAGLDIN) and Rev (LPPLRLTL) are similar to each other, but they show little resemblance to the CRT binding sites in α -integrin and the DNA recognition helix. One feature that is shared by most of these signals is the presence of hydrophobic amino acids that, when mutated, abrogates binding to CRT. In the case of the hydrophobic NES, the critical leucines are probably part of an amphipathic helix and the side chains are predicted to physically contact the receptors Crm1 and CRT. This is not the case for the two phenylalanines within the DNA recognition helix that are necessary for binding to CRT (3). The crystal structures of different nuclear receptors reveal that the phenylalanine side chains pack against the core of the DBD, at least when bound to DNA (32). Thus, the FF-to-AA mutations in the DNA recognition helix of GR that inhibit nuclear export probably affect the folding of the DBD, resulting in a structure that is no longer recognized by CRT (3).

How does CRT recognize its substrates? Our present study and previous work from other laboratories suggest that the N-terminal domain mediates substrate recognition and that regulation of binding is imparted by the Ca^{2+} -dependent conformational changes in the P-domain and C-terminal domain of CRT. Multiple low-affinity Ca^{2+} binding sites are contained within the C-terminal domain of CRT, and at least one high-affinity Ca^{2+} binding site is contained in the middle domain (P-domain) (2). Ca^{2+} is a cofactor for CRT binding to oligosaccharides, glycoproteins, and certain nonglycosylated proteins in vitro (43). Moreover, in our assays, Ca^{2+} is necessary for the physical interaction between CRT and the DBD as

TG and chelation with BAPTA-AM results in significant reduction of GR export to the cytoplasm. (C) Depletion of luminal Ca^{2+} stores does not inhibit NES export. The RGG 2.2 cell line expressing Rev-GFP was treated with Dex to induce importing of the reporter, which concentrates in the nucleoli. The cells were then maintained for 6 h under conditions that deplete Ca^{2+} . During the last 1 h, Dex was removed to allow Rev-GFP export to the cytoplasm. Rev-GFP export was observed whether or not Ca^{2+} was depleted.

measured by direct binding and as assayed by nuclear export of GR in permeabilized cells.

Ca^{2+} binding induces structural changes in CRT that dramatically alter its fragmentation pattern that results when it is treated with several different proteases (7). Of particular relevance to our study is the N-terminal 27 kDa of CRT, which is protected from tryptic digestion in the presence of Ca^{2+} but is highly susceptible in the absence of Ca^{2+} (7). This protease-resistant core of CRT retains at least one high-affinity Ca^{2+} binding site from the P-domain, while all of the low-affinity Ca^{2+} binding sites in the C-terminal domain are removed by digestion. We found that a CRT deletion mutant (residues 1 to 273) that contains the protease-resistant core is still functional for nuclear export of GR in permeabilized cells, indicating that the low-affinity Ca^{2+} binding sites are dispensable for our assays that score a positive interaction between CRT and GR. It is interesting that this CRT deletion mutant (residues 1 to 273) shows some Ca^{2+} -independent binding to the DBD, although the high-affinity Ca^{2+} binding site is still present in this mutant. The fact that the C-terminal Ca^{2+} binding sites are necessary for EGTA-induced inhibition of CRT binding to the DBD strongly suggests that the C-terminal domain functions in negative regulation of substrate binding. We have also observed that the N-terminal domain of CRT (residues 1 to 150) expressed as a GST fusion protein is sufficient to mediate nuclear export of GR in permeabilized cells (unpublished observations). This is consistent with previous data showing that the N-terminal domain of CRT can block GR binding to the GRE *in vitro* (6). All available information indicates, therefore, that the N-terminal domain of CRT is the substrate binding domain that physically contacts the DBD of GR. We infer that the N-terminal domain also binds hydrophobic NES substrates, since the DBD and NES display competitive interactions with CRT in our binding assays.

Emerging structural information provides a context for interpreting how Ca^{2+} might regulate CRT activity. Although the atomic structure of CRT has not yet been solved, the structure of the luminal domain of calnexin, which is 35% identical to CRT, has been solved at 2.9 Å resolution (37). The structure of calnexin reveals that it contains a compact globular domain (residues 61 to 262 and 415 to 458) and a large hairpin that forms a highly extended arm (residues 277 to 410). Tandem repeats in the P-domain comprise the arm, which projects 140 Å away from globular domain. The hairpin structure brings the N- and C-terminal domains together to form the globular domain (37). Thus, the close proximity of these domains may help explain how the occupancy of Ca^{2+} binding sites in the C-terminal domain can influence substrate recognition by the N-terminal domain in both calnexin and CRT. The nuclear magnetic resonance spectroscopy structure of the P-domain of CRT (residues 189 to 288) was recently solved, and, like calnexin, this domain forms a highly extended arm (9). The crystal structure of calnexin and the nuclear magnetic resonance spectroscopy structure of the P-domain of CRT were both solved in the presence of Ca^{2+} , and so the basis of Ca^{2+} -dependent changes in structure awaits further studies. It has been suggested that the P-domain or arm is a Ca^{2+} -sensitive protein interaction site for CRT (9).

Does Ca^{2+} regulate the engagement of CRT with nuclear export substrates? Both cytoplasmic and nuclear Ca^{2+} levels

can respond to signaling events, and in some cases the modulation of nuclear Ca^{2+} occurs independently of cytoplasmic Ca^{2+} (36). Depending on the system and method of measurement, Ca^{2+} levels in the cell are thought to increase to approximately micromolar concentrations on stimulation (5). This concentration would be predicted to fill the high-affinity Ca^{2+} binding sites on CRT but not the low-affinity sites. It should be noted, however, that the affinity of CRT for Ca^{2+} was measured *in vitro*. While it is clear that CRT contains at least two classes of binding sites with different affinities for Ca^{2+} , demonstrating the Ca^{2+} occupancy of particular sites on CRT in the cell may require the development of fluorescence-based assays that can register Ca^{2+} binding. This approach could be used to determine if Ca^{2+} is constitutively bound to CRT or if Ca^{2+} binds reversibly, thereby acting as a regulator of CRT function. We speculate that transient increases in Ca^{2+} concentration, theoretically, could promote the assembly of CRT-DBD complexes in the nucleus. The complex could then undergo export to the cytoplasm, where the complex is disassembled; which would be favored by low free Ca^{2+} concentrations.

Although the origin of nuclear Ca^{2+} remains an issue of debate, it is clear that processes including transcription are regulated by nuclear Ca^{2+} (16). Several observations are actually consistent with the notion that Ca^{2+} gradients between the nucleus and cytoplasm might be used to promote the assembly and disassembly of CRT complexes. First, the presence of Ca^{2+} ATPases in the nuclear envelope and the lack of Ca^{2+} buffering and sequestration proteins in the nucleus should prolong the availability of free Ca^{2+} (12). Second, the inner membrane of the nuclear envelope contains both major Ca^{2+} release channels, which may be activated independently of channels in the ER membrane that face the cytoplasm (36). Third, morphological data show that the ER forms invaginations that reach deep into the nucleus (13), which could place Ca^{2+} release channels close to sites of CRT-DBD assembly in the nucleoplasm. While it is clear that Ca^{2+} levels in the nucleus do change in response to signaling events, it remains to be established whether Ca^{2+} regulation of CRT is a dynamic process that involves reversible binding or whether Ca^{2+} is constitutively bound and simply maintains the tertiary structure of CRT.

CRT is thought to function in multiple pathways in the cell (23). In the ER, CRT may function as (i) a chaperone that mediates folding by transiently binding to oligosaccharide side chains and peptide domains, (ii) a Ca^{2+} storage protein involved in Ca^{2+} homeostasis, and (iii) a factor that directly regulates the activity of the Ca^{2+} pumps. At the plasma membrane, CRT may modulate (i) cell migration by interacting with adhesion plaque proteins and (ii) cell-cell interactions by interacting with cell surface proteins. In the nucleocytoplasmic compartment, CRT can regulate (i) the activity of steroid receptors through direct binding to the DBD of these proteins and (ii) the redistribution of steroid receptors to the cytoplasm. Because most of these functions mentioned above have been linked to the Ca^{2+} binding activity of CRT, conditions that influence the Ca^{2+} levels are predicted to regulate the activity of CRT. In this regard, our findings that Ca^{2+} is necessary for the nuclear export function of CRT *in vitro* and that Ca^{2+} depletion results in GR export defects *in vivo* suggest that this

pathway is used to regulate the nucleocytoplasmic distribution of GR and possibly other steroid hormone receptors. This link between Ca^{2+} and GR export could negatively regulate transcription through a nuclear transport pathway, perhaps using Ca^{2+} as a second messenger.

ACKNOWLEDGMENTS

We thank Gordon Hager, Dona Love, and John Hanover for cell lines and Ian Macara, Dirk Görlich, and Larry Gerace for plasmids.

Financial support was provided by the NIH (GM58639-01 to B.M.P.) and the DOD (DAMD 17-00-1-0048 to F.R.).

REFERENCES

- Askjaer, P., T. H. Jensen, J. Nilsson, L. Englmeier, and J. Kjems. 1998. The specificity of the CRM1-Rev nuclear export signal interaction is mediated by RanGTP. *J. Biol. Chem.* 273:33414-33422.
- Baksh, S., and M. Michalak. 1991. Expression of calreticulin in *Escherichia coli* and identification of its Ca^{2+} binding domains. *J. Biol. Chem.* 266: 21458-21465.
- Black, B. E., J. M. Holaska, F. Rastinejad, and B. M. Paschal. 2001. DNA binding domains in diverse nuclear receptors function as nuclear export signals. *Curr. Biol.* 11:1749-1758.
- Black, B. E., L. Lévesque, J. M. Holaska, T. C. Wood, and B. M. Paschal. 1999. Identification of an NTF2-related factor that binds Ran-GTP and regulates nuclear protein export. *Mol. Cell. Biol.* 19:8616-8624.
- Brini, M., and E. Carafoli. 2000. Calcium signalling: a historical account, recent developments and future perspectives. *Cell Mol. Life Sci.* 57:354-370.
- Burns, K., B. Duggan, E. A. Atkinson, K. S. Famulski, M. Nemer, R. C. Bleackley, and M. Michalak. 1994. Modulation of gene expression by calreticulin binding to the glucocorticoid receptor. *Nature* 367:476-480.
- Corbett, E. F., K. M. Michalak, K. Oikawa, S. Johnson, L. D. Campbell, P. Eggleton, C. Kay, and M. Michalak. 2000. The conformation of calreticulin is influenced by the endoplasmic reticulum lumenal environment. *J. Biol. Chem.* 275:27177-27185.
- Dedhar, S., P. S. Rennie, M. Shago, C. Y. Hagesteijn, H. Yang, J. Filmus, R. G. Hawley, N. Bruchovsky, H. Cheng, R. J. Matusik, and V. Giguere. 1994. Inhibition of nuclear hormone receptor activity by calreticulin. *Nature* 367: 480-483.
- Ellgaard, L., R. Riek, T. Herrmann, P. Peter Güntert, D. Braun, A. Helenius, and K. Wüthrich. 2001. NMR structure of the calreticulin P-domain. *Proc. Natl. Acad. Sci. USA* 98:3133-3138.
- Fischer, U., J. Huber, W. C. Boelens, I. W. Mattaj, and R. Luhrmann. 1995. The HIV-1 Rev activation domain is a nuclear export signal that accesses an export pathway used by specific cellular RNAs. *Cell* 82:475-483.
- Fornerod, M., M. Ohno, M. Yoshida, and I. W. Mattaj. 1997. CRM1 is an export receptor for leucine-rich nuclear export signals. *Cell* 90:1051-1060.
- Fox, J. L., A. D. Burgstahler, and M. H. Nathanson. 1997. Mechanism of long-range calcium signalling in the nucleus of isolated rat hepatocytes. *Biochem. J.* 326:491-495.
- Fricker, M., M. Hollinshead, N. White, and D. Vaux. 1997. Interphase nuclei of many mammalian cell types contain deep, dynamic, tubular membrane-bound invaginations of the nuclear envelope. *J. Cell Biol.* 136:531-544.
- Görlich, D., and U. Kutay. 1999. Transport between the cell nucleus and the cytoplasm. *Annu. Rev. Cell Dev. Biol.* 15:607-660.
- Greber, U. F., and L. Gerace. 1995. Depletion of calcium from the lumen of endoplasmic reticulum reversibly inhibits passive diffusion and signal-mediated transport into the nucleus. *J. Cell Biol.* 128:5-14.
- Hardingham, G. E., S. Chawla, C. M. Johnson, and H. Bading. 1997. Distinct functions of nuclear and cytoplasmic calcium in the control of gene expression. *Nature* 385:260-265.
- Helenius, A., T. S. Trombetta, D. N. Hebert, and J. F. Simons. 1997. Calnexin, calreticulin, and the folding of glycoproteins. *Trends Cell Biol.* 7:193-200.
- Holaska, J. M., B. E. Black, D. C. Love, J. A. Hanover, J. Leszyk, and B. M. Paschal. 2001. Calreticulin is a receptor for nuclear export. *J. Cell Biol.* 152:127-140.
- Holaska, J. M., and B. M. Paschal. 1998. A cytosolic activity distinct from Crm1 mediates nuclear export of protein kinase inhibitor in permeabilized cells. *Proc. Natl. Acad. Sci. USA* 95:14739-14744.
- Johnson, S., M. Michalak, M. Opas, and P. Eggleton. 2001. The ins and outs of calreticulin: from the ER lumen to the extracellular space. *Trends Cell Biol.* 11:122-129.
- Katagiri, Y., K. Takeda, Z. X. Yu, V. J. Ferrans, K. Ozato, and G. Guroff. 2000. Modulation of retinoid signalling through NGF-induced nuclear export of NGF1-B. *Nat. Cell Biol.* 2:435-440.
- Kehlenbach, R. H., A. Dickmanns, A. Kehlenbach, T. Guan, and L. Gerace. 1999. A role for RanBP1 in the release of CRM1 from the nuclear pore complex in a terminal step of nuclear export. *J. Cell Biol.* 145:645-657.
- Krause, K. H., and M. Michalek. 1997. Calreticulin. *Cell* 88:439-443.
- Lindsay, M. E., J. M. Holaska, K. Welch, B. M. Paschal, and I. G. Macara. 2001. Ran-binding protein 3 is a cofactor for Crm1-mediated nuclear protein export. *J. Cell Biol.* 153:1391-402.
- Liu, J., and D. B. DeFranco. 2000. Protracted nuclear export of glucocorticoid receptor limits its turnover and does not require the exportin 1/CRM1-directed nuclear export pathway. *Mol. Endocrinol.* 14:40-51.
- Love, D. C., T. D. Sweitzer, and J. A. Hanover. 1998. Reconstitution Of HIV-1 Rev nuclear export-independent requirements for nuclear import and export. *Proc. Natl. Acad. Sci. USA* 95:10608-10613.
- McNally, J. G., W. G. Muller, D. Walker, R. Wolford, and G. L. Hager. 2000. The glucocorticoid receptor: rapid exchange with regulatory sites in living cells. *Science* 287:1262-1265.
- Nakielnny, S., and G. Dreyfuss. 1999. Transport of proteins and RNAs in and out of the nucleus. *Cell* 99:677-690.
- Ostwald, T. J., and D. H. MacLennan. 1974. Isolation of a high affinity calcium-binding protein from sarcoplasmic reticulum. *J. Biol. Chem.* 249: 974-979.
- Paschal, B. M., and L. Gerace. 1995. Identification of NTF2, a cytosolic factor for nuclear import that interacts with nuclear pore complex protein p62. *J. Cell Biol.* 129:925-937.
- Picard, D., and K. R. Yamamoto. 1987. Two signals mediate hormone-dependent nuclear localization of the glucocorticoid receptor. *EMBO J.* 6:3333-3340.
- Rastinejad, F. 2001. Retinoid X receptor and its partners in the nuclear receptor family. *Curr. Opin. Struct. Biol.* 11:33-38.
- Rojiani, M. V., B. B. Finlay, V. Gray, and S. Dedhar. 1991. In vitro interaction of a polypeptide homologous to human Ro/SS-A antigen (calreticulin) with a highly conserved amino acid sequence in the cytoplasmic domain of integrin alpha subunits. *Biochemistry* 30:9859-9866.
- Rubio, I., P. Buckle, H. Trutnau, and R. Wetzker. 1997. Real-time assay of the interaction of a GST fusion protein with a protein ligate using resonant mirror technique. *Bio/technology* 22:269-271.
- Saito, Y., Y. Ihara, M. R. Leach, M. F. Cohen-Doyle, and D. B. Williams. 1999. Calreticulin functions in vitro as a molecular chaperone for both glycosylated and non-glycosylated proteins. *EMBO J.* 18:6718-6729.
- Santella, L., and K. Kozuka. 1997. Effects of 1-methyladenine on nuclear calcium transients and meiosis resumption in starfish oocytes are mimicked by the nuclear injection of inositol 1,4,5-triphosphate and cADP-ribose. *Cell Calcium* 22:11-20.
- Schrag, J. D., J. J. Bergeron, Y. Li, S. Borisova, M. Hahn, D. Y. Thomas, and M. Cygler. 2001. The structure of calnexin, an ER chaperone involved in quality control of protein folding. *Mol. Cell* 8:633-644.
- Singh, N. K., C. D. Atreya, and H. L. Nakhasi. 1994. Identification of calreticulin as a rubella virus RNA binding protein. *Proc. Natl. Acad. Sci. USA* 91:12770-12774.
- Stade, K., C. S. Ford, C. Guthrie, and K. Weis. 1997. Exportin 1 (Crm1p) is an essential nuclear export factor. *Cell* 90:1041-1050.
- Steggerda, S. M., and B. M. Paschal. 2002. Regulation of nuclear import and export by the GTPase Ran. *Int. Rev. Cytol.* 217:41-91.
- Stoffler, D., K. N. Goldie, B. Feja, and U. Aebi. 1999. Calcium-mediated structural changes of native nuclear pore complexes monitored by time-lapse atomic force microscopy. *J. Mol. Biol.* 287:741-752.
- Strubing, C., and D. E. Clapham. 1999. Active nuclear import and export is independent of lumenal Ca^{2+} stores in intact mammalian cells. *J. Gen. Physiol.* 113:239-248.
- Vassilakos, A., M. Michalak, M. A. Lehrman, and D. B. Williams. 1998. Oligosaccharide binding characteristics of the molecular chaperones calnexin and calreticulin. *Biochemistry* 37:3480-3490.
- Wen, W., J. L. Meinkoth, R. Y. Tsien, and S. S. Taylor. 1995. Identification of a signal for rapid export of proteins from the nucleus. *Cell* 82:463-473.
- Wente, S. R. 2000. Gatekeepers of the nucleus. *Science* 288:1374-1377.
- Wiechens, N., and F. Fagotto. 2001. CRM1- and Ran-independent nuclear export of beta-catenin. *Curr. Biol.* 11:18-27.

Structural Basis for Bile Acid Binding and Activation of the Nuclear Receptor FXR

Short Article

Li-Zhi Mi,¹ Srikripa Devarakonda,¹

Joel M. Harp,² Qing Han,¹ Roberto Pellicciari,³

Timothy M. Willson,⁴ Sepideh Khorasanizadeh,²
and Fraydoon Rastinejad^{1,2,*}

¹Department of Pharmacology

²Department of Biochemistry and Molecular Genetics
University of Virginia Health System
Charlottesville, Virginia 22908

³Università Di Perugia

Departimento di Chimica e Tecnologia del Farmaco
06123 Perugia
Italy

⁴Discovery Research
GlaxoSmithKline

Research Triangle Park, North Carolina 27709

Summary

The nuclear receptor FXR is the sensor of physiological levels of enterohepatic bile acids, the end products of cholesterol catabolism. Here we report crystal structures of the FXR ligand binding domain in complex with coactivator peptide and two different bile acids. An unusual A/B ring juncture, a feature associated with bile acids and no other steroids, provides ligand discrimination and triggers a π -cation switch that activates FXR. Helix 12, the activation function 2 of the receptor, adopts the agonist conformation and stabilizes coactivator peptide binding. FXR is able to interact simultaneously with two coactivator motifs, providing a mechanism for enhanced binding of coactivators through intermolecular contacts between their LXXLL sequences. These FXR complexes provide direct insights into the design of therapeutic bile acids for treatment of hyperlipidemia and cholestasis.

Introduction

Bile acids are the endogenous ligands for FXR, the nuclear receptor that transcriptionally regulates their production, movement, and absorption (Chawla et al., 2001; Goodwin and Kliever, 2002; Lu et al., 2001). As the end products of hepatic cholesterol catabolism, bile acid production is intimately linked to cholesterol homeostasis. In humans, inherited genetic defects associated with the impairment of bile acid homeostasis lead to severe cholestatic disease and vitamin absorption deficiency (Achord, 1990; Hofmann, 1999a, 1999b). Due to its role in the regulation of cholesterol and bile acid levels, FXR is a potential drug target for treatment of hyperlipidemia and cholestatic disease. To understand the mechanism of bile acid binding and activation in FXR, we solved two crystal structures of its ligand binding domain (LBD) in the presence of a GRIP-1 coactivator peptide. One structure contains the high-affinity bile acid 6 α -ethylchenodeoxycholic acid (6ECDCA) solved at 2.5 Å resolution,

and the second structure contains 3-deoxyCDCA, solved at 2.9 Å resolution (Table 1). Together, these structures show how the physiological activities of bile acids are dictated by the chemical composition of their unique steroid skeleton.

Results and Discussion

Overall Architecture of FXR

The FXR protein was expressed from *E. coli* with a N-terminal polyhistidine tag and purified as described in the Experimental Procedures. Crystals of FXR bound to 6ECDCA or 3-deoxyCDCA were obtained under the same conditions. These crystals exhibited identical crystallographic parameters and showed the same molecular arrangements of FXR (Table 1). The asymmetric units contain two representations of the FXR, herein referred to as the *a*' and the *b* complexes, which differed in the number of coactivator peptides bound to FXR (one peptide in the *a* complex, two peptides in the *b* complex). Figures 1–3 show the overall disposition of the LBD, the ligand and coactivator peptides from the 6ECDCA crystal. The electron density maps clearly show that the A ring of the bile acid faces the C-terminal helix 12, the activation function 2 (AF2) of the receptor (Figures 1 and 2A). This orientation was unanticipated, as progesterone, estrogen, testosterone, and glucocorticoids are all oriented in the opposite direction with their D rings facing helix 12 of their respective receptors (Bledsoe et al., 2002; Brzozowski et al., 1997; Sack et al., 2001; Shiau et al., 1998; Williams and Sigler, 1998). Bile acid binding directly places helix 12 against helices 3, 4, and 10 (Figure 1). This receptor conformation represents the "activated" state, whereby helix 12 stabilizes the binding of coactivator peptide (Figures 1A and 3A).

Bile Acid Binding and Discrimination

Bile acids are water-soluble amphipathic steroids that play important roles in cholesterol disposal and intestinal lipid absorption through micelle formation. The physicochemical properties of the bile acid skeleton are essential in this regard, displaying a convex hydrophobic face and a concave hydrophilic face. The steroid nucleus in bile acids is not flat, due to a hydrogen atom at C5 oriented in the β configuration (Figures 1C and 2A). This substituent causes the A/B ring juncture to be *cis*, forcing ring A to lie outside of the plane of the BCD ring system. As a result, the separation between the 3 α -OH and the C-24 carboxylate of CDCA (14 Å) is substantially shorter than the contour length of the molecule (21 Å), giving bile acids a rounded profile that allows a close fit with respect to the pocket in FXR (Figures 1B and 1C). Figures 1B and 1C show how the shape of the FXR ligand binding pocket complements the nonplanar bile acid skeleton.

The FXR ligand binding pocket also utilizes the amphipathic properties of the bile acids to provide additional molecular recognition beyond their unique shape. Bile acids contain distinct α and β faces. The β face is com-

*Correspondence: fr9c@virginia.edu

Table 1. Crystallographic Data and Refinement Statistics

	6-ethyl-CDCA	3-deoxy-CDCA
Space group	P2 ₁ 2 ₁ 2	P2 ₁ 2 ₁ 2
Resolution (Å)	24.3–2.50 (2.59–2.50)	15.0–2.90 (3.0–2.9)
Unit cell dimension (a, b, c) (Å)	99.829 107.452 69.280	99.535 107.129 69.206
Unique reflections	24427	12668
Completeness (%)	92.8 (77.2)	98.9 (99.6)
Average redundancy	4.0 (3.4)	4.7 (4.8)
R _{sym} (%) ^a	4.4 (28.2)	7.1 (45.8)
R _{working} ^b	25.1	25.4
R _{free} ^c	28.1	29.0
Rms deviation bonds (Å)	0.010	0.011
Rms deviation angles (deg)	1.6	1.9
Rms dihedral angles (deg)	19.5	22.3
Rms improper angles (deg)	0.93	1.10

Values in parentheses are for the highest resolution shells.

^aR_{sym} = $\sum |I_h - \langle I_h \rangle| / \sum I_h$, where $\langle I_h \rangle$ is the average intensity over symmetry equivalent reflections.

^bR_{working} = $\sum ||F_o| - |F_c|| / \sum |F_o|$, where F_o and F_c are the observed and calculated structure-factor amplitudes.

^cR_{free} was calculated using 5% of data excluded from refinement.

posed of a continuous hydrocarbon surface punctuated with the angular methyl groups at C18 and C19 (Figure 1C). The primary and secondary bile acids contain a common β face, and a distinct α face on which hydroxyls are displayed in the 3 α , 7 α , and 12 α positions. The relative affinities of chenodeoxycholic acid (CDCA), deoxycholic acid (DCA), cholic acid (CA), and lithocholic acid (LCA) for FXR (Makishima et al., 1999; Parks et al., 1999; Wang et al., 1999) are dictated by their specific pattern of axial hydroxyl groups at the 7 and 12 positions. The side chain oxygen of Tyr366 hydrogen bonds with the axial 7 α -OH on ring B, and the lack of this hydroxyl in LCA lowers its affinity. Moreover, as the pocket does not provide any polar side chains to accommodate the 12 α -OH group on ring C, the binding of CA and DCA would be energetically costly in comparison to CDCA. The FXR structure also reveals pockets that are not entirely filled by substituents found on naturally occurring bile acids (Figure 1B and 1C). The semisynthetic bile acid 6ECDCA (Pellicciari et al., 2002) places the 6 α -ethyl group into one such hydrophobic cavity that exists between the side chains of Ile359, Phe363, and Tyr 366, accounting for its higher affinity.

The current structures also provide an explanation for how conjugated bile acids bind and activate FXR. Mammalian and nonmammalian bile acids are often amidated with glycine or taurine at the C24 carboxylate, and these conjugations are known to only modestly affect the binding affinity and activation efficacy (Makishima et al., 1999; Parks et al., 1999; Wang et al., 1999). The structure shows that the carboxylate oxygens of CDCA hydrogen bond with the guanidino group of Arg328 side chain located at the entry point of the pocket. The proximity of the carboxylate on the ligand to the solvent suggests that conjugated amino acids would be positioned completely out of the pocket and solvent exposed, thus not impacting receptor activation. Since amidation still preserves a carbonyl oxygen for hydrogen bonding with Arg328, the bile acid binding affinity would also remain largely unchanged.

As a sensor of physiological levels of enterohepatic bile acids, FXR binds to its cognate ligands with ~1000-fold weaker affinity than other steroid receptors bind to their cognate hormones, yet FXR shows remarkable

specificity for bile acids (Makishima et al., 1999; Parks et al., 1999; Wang et al., 1999). Figures 1B and 1C show that the steroid skeleton and the ligand pocket lack a sufficient number of hydrogen bond donors and acceptors to fully account for bile acid discrimination from other steroid hormones. Instead, the FXR ligand binding pocket has evolved to recognize bile acids both using their unique nonplanar shapes and amphipathic physicochemical properties.

The physical-shape discrimination mechanism employed by FXR for ligand binding precludes essentially all other steroids and cholesterol metabolites from acting on this receptor. Estrogens have an aromatic ring A and thus no possibility of *cis-trans* isomerism at carbon-5. Progesterone, aldosterone, glucocorticoids, and testosterone contain a 4-ene structure in ring A, and cholesterol contains a 5-ene in ring B, and therefore all lack the necessary 5 β hydrogen required to juncture A/B rings into *cis*. In addition to their differing shapes, none of these other molecules share the amphipathic and detergent-like properties uniquely associated with the α and β faces of bile acids that are both critical to their biological function and make their binding to FXR possible.

π -Cation Receptor Activation Trigger

All naturally occurring bile acids contain a *cis*-oriented A/B ring juncture and a 3 α -hydroxyl group in their A ring. The FXR structure shows the A ring and the 3-hydroxy group oriented toward helix 12 where they interact with the His444 on helix 10/11 and Trp466, the only residue from helix 12 in close proximity to the ligand (Figure 2A). These two residues function as the receptor's activation trigger through formation of a desolvated π -cation interaction directly contacted and stabilized by the bile acid (Figure 2A). The bile acid A ring also contacts Tyr358, which further restricts the position of His444. The π -cation interaction between the indole ring of a Trp (π electron system) and the Ne (cation) on a perpendicularly oriented His' side chain has been described in other biological systems but never observed as a molecular switch for receptor activation (Ma and Dougherty, 1997). We infer that in the absence of ligand, the same His-Trp interaction cannot be stabilized due to insufficient physical

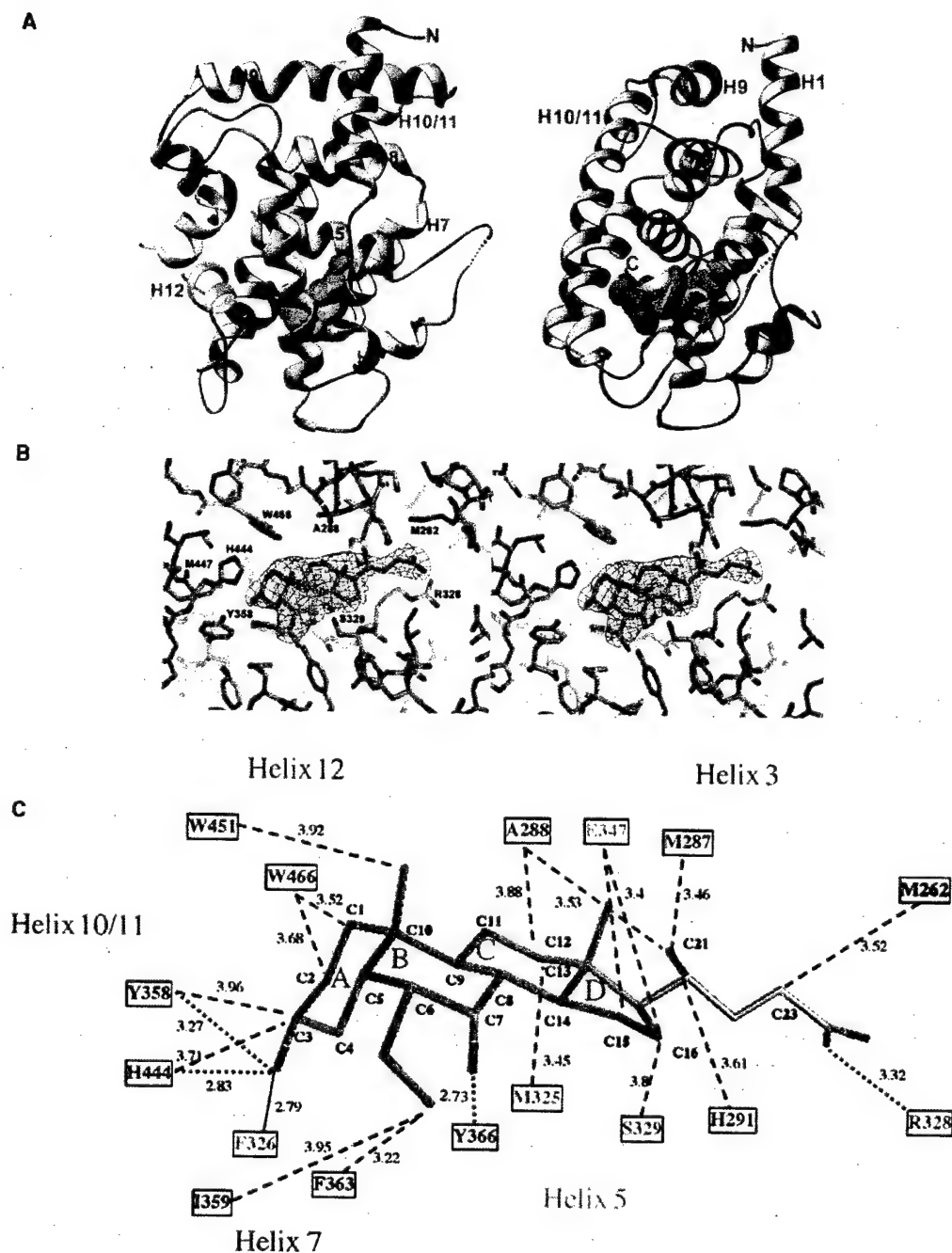


Figure 1. Overall Views of FXR and Its Ligand Interactions

(A) Perpendicular views of the FXR LBD (purple) from complex b of the 6ECDCA complex. Helix 12 of the receptor is shown in yellow, the GRIP-1 peptides are shown in blue and red, and 6ECDCA is shown in green.

(B) Stereo view of a simulated annealing omit electron density ($F_o - F_c$) map showing the bound 6ECDCA. The ligand was excluded in map calculation.

(C) Schematic representation of the FXR/6ECDCA interactions. Dotted red lines indicate hydrogen bonds; dotted blue lines indicate van der Waals contacts.

constraints on these residues. The loss of their interaction would remove the necessary support for helix 12 in its active position.

The 3α hydroxyl on ring A is the most polar functionality on the steroid nucleus due to its equatorial position

with respect to the hydrocarbon ring system (Figure 1C). To gauge the relative contributions to receptor activation from the 3-OH group versus the ring A surface, we studied 3-deoxyCDCA in biochemical assays and by X-ray crystallography. We found that the 3-deoxyCDCA

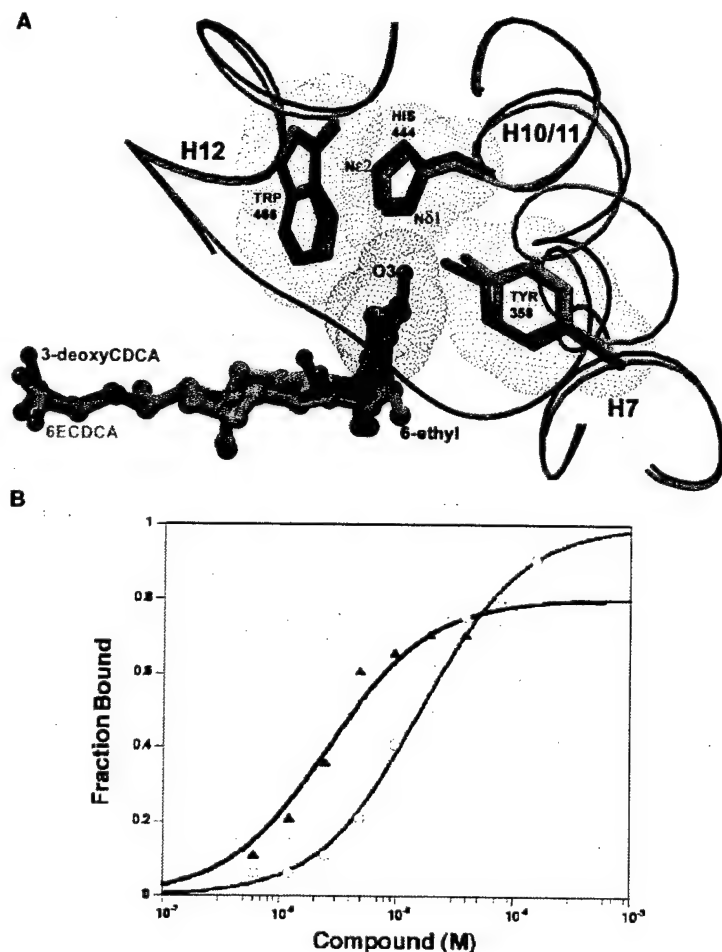


Figure 2. The Activation Mechanism of FXR
(A) 6ECDCA and 3-deoxyCDCA interactions with the activation switch of FXR. Shown is the superposition of their two crystal structures in the vicinity of the ligand and residues His444 and Trp466.
(B) The binding of GRIP-1 NID-3 coactivator peptide to FXR as a function of increasing 3-deoxyCDCA (black triangles) and CDCA (red circles).

is able to recruit the region-3 LXXLL motif of GRIP-1 with an EC_{50} of 3 μ M, in comparison to CDCA which shows an EC_{50} of 16 μ M (see Figure 2B). The small increase in potency is likely due to the decreased hydrophilicity of 3-deoxyCDCA, which aids desolvation of the ligand. These results suggested that the 3-hydroxyl alone is not responsible for activation of the receptor. To directly visualize how the 3-deoxy bile acid activates FXR, we solved the crystal structure of its complex and examined the ligand with respect to the activation trigger (Figure 2A). We found that ring A of the 3-deoxyCDCA still contacts and orients His444 and Trp466, allowing the same π -cation interaction as in the 6ECDCA complex. A hydrogen bond to the side chain nitrogen on His444, no longer available from the 3-OH of ring A, is instead donated by the side chain OH group of Tyr358. Overall, the structure shows helix 12 in the identical activated conformation seen in the 6ECDCA structure and still supporting the association of coactivator peptide. Therefore, a correctly positioned ring A is the dominant factor mediating the agonist function of bile acids.

A sequence alignment shows that the amino acids responsible for the binding of the sex steroids, glucocorticoids, and mineralocorticoids are more closely con-

served between their receptors than with FXR (Figure 4). Nevertheless, all of these receptors form their ligand binding pockets largely via determinants located on helices 3, 5, 7, 10/11, and 12. Importantly, every residue responsible for the binding of rat FXR to bile acids is identical in the human FXR protein (Figure 4). However, mouse FXR β , which is a pseudogene in humans, contains several differences at these residue positions but also appears to use lanosterol as its endogenous ligand (Otte et al., 2003). As the π -cation activation trigger had not been previously seen in other steroid receptors, we compared sequences in Figure 4 to look for the conservation of this pair of His and Trp residues. Besides the FXR proteins, LXR α and LXR β receptors are the only other receptors with identically positioned His and Trp residues (Figure 4). As LXR α and LXR β bind to oxysterols and regulate genes that are also related to cholesterol and bile acid homeostasis (Lu et al., 2001; Peet et al., 1998), these receptors may be activated via a similar π -cation molecular switch.

Coactivator Interactions

The GRIP-1 coactivator contains three separate nuclear receptor interaction domains (NIDs), each consisting of

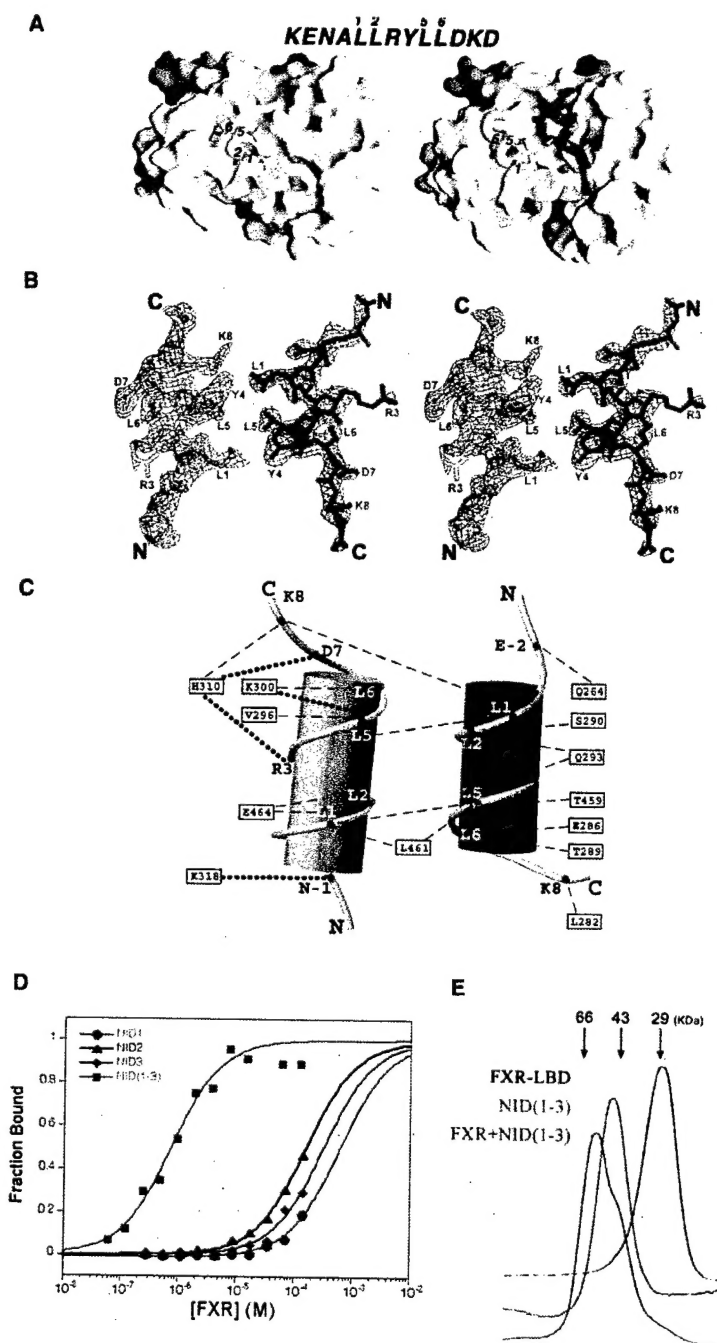


Figure 3. The Interaction of FXR with Coactivator

(A) Comparison of the *a* and *b* complexes in the asymmetric unit of the 6ECDCA structure. Helix 12 is shown in yellow, the peptide in the primary coactivator groove is shown in blue, and the second peptide seen in the *b* complex (of both the 6ECDCA and 3-deoxyCDCA containing structures) is shown in red. The numbers indicate the location of the conserved leucines.

(B) A section of a composite omit map (2Fo-Fc) showing electron density for the two coactivator peptides in complex *b*. The primary coactivator peptide is in blue; the second peptide is in red.

(C) A schematic representation showing the contacts of the primary coactivator peptide (blue) with the second peptide (red) and with FXR (residues indicated in boxes). Circles represent hydrogen bonds; dotted lines indicate van der Waals contacts.

(D) FXR binding to different NID regions of GRIP1 in the presence of CDCA. The NID-1 peptide has the sequence KGQTKLLQLLTTK, the NID-2 is EKHILHRLQLQDS, and the NID-3 is KENALLRYLLDKD. The NID (1-3) protein consists of the three consecutive NID regions of GRIP1.

(E) Gel filtration chromatography (Pharmacia 100 cm Superdex-75) showing the migration of FXR-LBD, the NID (1-3) region of GRIP-1, and the FXR-LBD + NID (1-3). The elution profiles are shown as a function of increasing time (left to right). The migration of several molecular weight standards is indicated at the top. FXR-LBD elutes at the expected size of a monomer (~29 kDa). The NID (1-3) polypeptide alone elutes at a larger size (~46 kDa) than expected (calculated mass ~24 kDa), presumably due to a noncompact fold. FXR-LBD + NID (1-3) migrates at a size of ~60 kDa, consistent with one FXR-LBD bound to a more compact NID (1-3) and not consistent with the cooperative binding of two FXR-LBDs subunits with one NID (1-3) fragment (expected migration at a size >82 kDa).

a LXXLL motif (Darimont et al., 1998; Xu et al., 1999). Synthetic peptides corresponding to NID-1, NID-2, and NID-3 regions bind to bile acid-activated FXR weakly, with NID-1 binding with $K_D > 500 \mu\text{M}$, NID-2 binding with K_D of ~160 μM , and NID-3 binding with K_D of ~330 μM (Figure 3B). The coactivator peptide in the structures is NID-3, with the sequence KENALLRYLLDKD. Both *a* and *b* complexes show a peptide binding in the primary activator groove as described for other receptors (Figure 3A) (Bledsoe et al., 2002; Brzozowski et al., 1997; Dari-

mont et al., 1998; Gampe et al., 2000; Nolte et al., 1998; Shiao et al., 1998). However, the *b* complexes of both the 6ECDCA and 3-deoxyCDCA structures show a second copy of NID-3 bound adjacent to the primary coactivator peptide (Figure 3A). This arrangement allows the two antiparallel NIDs to form cross interactions via their hydrophobic side chains in a manner that requires the agonist conformation of helix 12. The inability of the second peptide to occupy its site in complex *a* appears to be caused by the lack of the necessary access arising

rFXR	238	-----EKTELTVDQQTLLDYIMDSYSKQRM ^Q PQE-----ITNKILKEEFSAE--	
hFXR	245	-----EKTELTDPQQTLLHFINDSYNKQRM ^Q PQE-----ITNKILKEEFSAE--	
mFXR β	241	-----DNMTLTQEEHRLNTIVTAHQKSMIPLG-----ETSKLLQEGSNPE--	
VDR	118	-----DSLRLPKLSEEQRIIAILLDAHHKT ^V DPT ^V SD ^F CQFRPPVRVNDGGGSVTLELS	
LXR α	205	-----QLSPEQLGMIKLVAAQQQCNRRSFSDRL-----RVTPWPMPADPHSREA	
LXR β	219	-----QLTAAQELMIQQLVAAQLOCNKRSFSQDQ-----KVTPWPLGADPQSRDA	
AR	667	-----YECQPIFLNVLEAIEPGVVCAGH-----DNNQPDSD	
PR	682	-----QLIPPLINLLMSIEPDVIYAGH-----DNTKPDPT	
ER	301	-----SKKNSLALSLTADQMVSAALLDAEPPIYSEY-----DPTRPFS	
GR	527	-----QLTPTLVSLLEVIEPEVLYAGY-----DSSVPDS	
MR	719	VNTALVPQLSTISRALTSPVMVLENIEPEIKAGY-----DSSKPDT	
helix-1 helix-2			
rFXR	279	--ENFLILTE ^M ATS ^H VQ ^L FLVEFTKRLPGFQTL ^D H ^Q QIALLK ^S SAVEAM ^F LRS ^A E ^I FNK-	
hFXR	286	--ENFLILTEMATNHVQ ^L FLVEFTKKLPGFQTL ^D HEDQ ^I ALLKGS ^S SAVEAM ^F LRS ^A E ^I FNK-	
mFXR β	282	--LSFLRLSESVLHIC ^L MLMKFTKGLPGFENLT ^T EDQ ^A ALQKASKTEVM ^F LHVA ^L QLYGGK	
VDR	224	QLSM ^L PH ^L AD ^L VSY ^S ISIQ ^V IGFAPKMI ^P GRDLT ^S EDQ ^I VLLKSSA ^I EV ^I MA ^R SNES ^F TMD	
LXR α	240	RQORFAHFTELAIVSVQ ^E IVDFAKQ ^L PGFLQ ^L SR ^E DQ ^I ALLKTS ^A IEVM ^L LET ^S RRYNP-	
LXR β	264	RQORFAHFTELAII ^S VQ ^E IVDFAKQ ^V PGFLQ ^L GR ^E DQ ^I ALLKASTIEIM ^L LET ^S ARRYNH-	
AR	697	FAAL ^L SS ^L NE ^L IGER ^L LVHVV ^K AKAL ^P GFRLNH ^V DDQ ^M AVIQ ^S WM ^L GL ^M V ^F AM ^G WR ^S FTN	
PR	711	SSSL ^L TS ^L LN ^L Q ^L GER ^L LLSV ^V KWSK ^L PGFRNLH ^I DDQ ^I TLIQ ^S WM ^L SL ^M V ^F GL ^M WR ^S YKH	
ER	339	EAS ^M GL ^L TN ^L LA ^D R ^L LVHMIN ^W AKR ^V PGFV ^D LT ^L HDQ ^V HLL ^E CAW ^L E ^I LM ^I GL ^V WR ^S MEH	
GR	556	TWRI ^M TT ^L NN ^L LC ^R Q ^V IAAV ^K WAKA ^I PGFRNLH ^L DDQ ^M TLQ ^S WM ^L FL ^M A ^F GL ^M WR ^S YRQ	
MR	762	AENLL ^S TLN ^R LAG ^K QMIQ ^V V ^V KWAK ^V LP ^G FKNL ^P LEDQ ^I TLIQ ^S WM ^L CL ^S SS ^F AL ^S WR ^S YKH	
helix-3 helix-3' helix-4 helix-5			
rFXR	336	-----KLPAGHADLL--EE ^I IRKS-----GISDE ^V ITP ^M FS ^F Y	
hFXR	343	-----KLPSGHSDLL--EE ^I IRNS-----GISDE ^V ITP ^M FS ^F Y	
mFXR β	340	DSTSGSTMRPAKPSAG ^T LEVHNP ^S ADESV ^H SPEN ^F LKEGY ^S APL ^T DIT ^K EFIAS ^L SYFY	
VDR	283	-----DMS ^M T ^C GNQDY ^K YRVSD ^V TK ^A -----GH ^S LE ^L IEP ^T IK ^F Q	
LXR α	309	-----GSEIT ^F LKDFS ^N RED ^F AKA-----GLQ ^V EFIN ^P IF ^E FS	
LXR β	323	-----ETECIT ^F LKDF ^T YSKDD ^F HRA-----GLQ ^V EFIN ^P IF ^E FS	
AR	757	-----VNSRMLY ^F APDL ^V FNE ^Y RMHK-----SR ^M YSQ ^C VR ^M RL ^S	
PR	771	-----VSGQMLY ^F APDL ^L ILNE ^Q RMKE-----SSF ^S Y ^S CL ^T MQ ^W IP	
ER	399	-----PVKLL ^F APNLL ^L DRN ^Q GKCV-----EG ^M VE ^T FD ^M LL ^A TS	
GR	616	-----SSANLLC ^F APDL ^I INE ^Q RMT-----L-PCMYD ^C CKH ^M LY ^V S	
MR	822	-----TNSQFLY ^F APDL ^V FNE ^E KMH-----Q-----SAMYELC ^Q GMH ^Q IS	
beta-3 beta-4 helix-6 helix-7			
rFXR	367	KSVGELKMTQ ^E EA ^L LT ^A IVILSPD-----RQYIKDREAVEK ^L QEP ^L LDVL ^Q KLCKI	
hFXR	374	KSGELKMTQ ^E EE ^V AL ^T IVILSPD-----RQYIKDREAVEK ^L QEP ^L LDVL ^Q KLCKI	
mFXR β	400	RRMSELHVS ^D TEY ^L LT ^A TTVL ^F SD-----RPCLKNK ^Q HIE ^N LQEP ^V LQL ^L FK ^F SKM	
VDR	318	VGLKKLNLH ^E EEH ^V LLMA ^I CIVSPD-----RPGVQDAALIE ^A IQDR ^L SNT ^L QTY ^I RC	
LXR α	344	RANNE ^L QLN ^D AE ^F AL ^I AI ^S IFSAD-----RPNVQDQ ^L QVER ^L QHTY ^V EALHAY ^V SI	
LXR β	358	RAMRRLGLDDA ^E YAL ^I AINIFSAD-----RPNVQEPGR ^V EALQ ^Q PYVEAL ^L SY ^T RI	
AR	792	QEPGWLQITPQ ^E FLCM ^K ALL ^L FS ^I IP-----VDGLKNQ ^K FF ^D ELRM ^N YIKEL ^D RI ^I AC	
PR	806	QEPVKLQVSQ ^E EEFLCM ^K VLL ^L NTIP-----LEGLRSQ ^T QFE ^M RSSY ^I REL ^I KA ^I GL	
ER	433	SRFRMNNLQ ^G EEFVCL ^S IILL ^N SGVY ^T FLS ^S TLKS ^L EED ^H IHRV ^L DKIT ^D TLI ^L MA ^K	
GR	651	SELHRLQVS ^Y EEYLC ^M KTLL ^L SS ^V P-----KDGLKSQ ^E LF ^D EIR ^M TYIKEL ^G KA ^I VK	
MR	857	LQFVRLQ ^L T ^F EYTIM ^K VLL ^L STIP-----KDGLKSQ ^A A ^F EEM ^R TNYIKEL ^R KM ^V TK	
helix-8 helix-9			
rFXR	419	YQ---PENPQH ^F ACLLGR ^L TEL ^R T ^F NNH ^H AE ^M LM ^S WRV ^N ---DHKFT ^P LLCE ^I WDVQ--	
hFXR	426	HQ---PENPQH ^F ACLLGR ^L TEL ^R T ^F NNH ^H AE ^M LM ^S WRV ^N ---DHKFT ^P LLCE ^I WDVQ--	
mFXR β	452	YH---PEDPQH ^F ACLLGR ^L TEL ^R TL ^S HS ^H SEIL ^R MW ^K T---D ^P RLV ^M LF ^S EK ^W DL ^H S ^F	
VDR	370	RH-PPGSHLLYAKMIQ ^K LAD ^L RLS ^N EE ^S KQ ^V Y ^R CL ^S FQ ^E C-SM ^K LT ^P L ^V LE ^V E ^G NE ^I S	
LXR α	396	HH---PHDRLM ^F PRML ^M KLV ^S LR ^T LSS ^V HSEQ ^V FAL ^R LQ---DKKL ^P PLL ^S EI ^W DV ^H E-	
LXR β	410	KR---PDQ ^L LR ^F PRML ^M KLV ^S LR ^T LSS ^V HSEQ ^V FAL ^R LQ---DKKL ^P PLL ^S EI ^W DV ^H E-	
AR	845	KRK ^N PTSC ^S RRFYQ ^L TKL ^L DSV ^Q PIARE ^H Q ^F FD ^L L ^I KSH ^M V ^S VD ^F PE ^M MAE ^I SVQ ^V P	
PR	859	RQKGVVSS ^S QRFYQ ^L TKL ^L DN ^L HD ^L VK ^Q LH ^L Y ^C LN ^F IQ ^S RAL ^S VE ^F PE ^M SE ^V IAA ^Q LP	
ER	493	AGTLQQQH ^Q RLAQL ^L LL ^L SHIR ^H MSN ^K Q ^M HL ^Y SM ^K CKN---VVPLYD ^L LL ^L EM ^L DA ^H RL	
GR	704	REGNSQN ^Q WRFYQ ^L TKL ^L DSM ^H EV ^V EN ^L NY ^C FQ ^T FLD-KTMS ^L FE ^F PE ^M LA ^E ILT ^N Q ^I P	
MR	910	CPNNSGQ ^S WQRFYQ ^L TKL ^L DSM ^H DL ^V SD ^L LE ^F CFY ^T FRESH ^A LK ^V EP ^F AML ^V EI ^I SD ^Q LP	
helix-10/11 helix-12 (AF2)			
mFXR β	505	S-----	
AR	905	KILSGKVK ^P IY ^F HTQ-----	
PR	919	KILAGMVK ^P LL ^F HKK-----	
ER	550	HAPTSRGGASVEETDQ ^S HLATAG ^S TSS ^H SLQ ^K YVITGEA ^E GFPATV	
GR	763	KYSNGNIKK ^L LF ^H QK-----	
MR	971	KVESGNAK ^P LY ^F HRK-----	

Figure 4. Sequences Used for Ligand Binding by the Steroid Receptors

Yellow shading shows the position of the α helices; blue shows β strands. Red boxes indicate the residues that contact the steroids as determined from crystal structures (Bledsoe et al., 2002; Brzozowski et al., 1997; Rochel et al., 2000; Sack et al., 2001; Shiao et al., 1998; Williams and Sigler, 1998), and black ovals indicate the residues involved in the π -cation molecular switch for ligand-induced activation of FXR. All of the residues in rFXR that contact CDCA-derived ligands are identical with human FXR but not as closely shared with mFXR β , which has been shown to respond to lanosterol (Otte et al., 2003). The crystal structures of hFXR, mFXR β , LXR α , LXR β , and MR are unavailable.

from a crystal packing effect involving a symmetry related subunit. Figure 3B shows the electron density maps for both peptides in complex *b*, and Figure 3C shows a schematic drawing of these peptide-peptide and peptide-FXR contacts.

Within the NID-3 LXXLL motif, Arg3 and Tyr4 (occupying the XX positions) are not conserved among the coactivator NIDs and are solvent exposed in the complexes described here (Figure 3A). By contrast, Leu2 and Leu6, which are highly conserved in coactivator NIDs, are responsible for forming the peptides' contacts to FXR (Figure 3C). Leu5 forms the peptide-peptide interactions with Leu1 in the *b* complexes (Figures 3A and 3C). Through the two sets of Leu5/Leu1 interactions, the binding of one peptide enhances the binding of the second peptide by providing a more favorable interaction site. These peptide-peptide interactions would suggest that two NIDs contained within the same polypeptide should bind to FXR with significantly higher affinity, due to the constraints on their physical freedom.

Figure 3B shows that an extended GRIP-1 region (NID [1-3]) that contains more than one NID motif does in fact bind to the FXR more with 100 times greater strength (K_D 0.8 μ M) than any of its isolated NID elements. This higher affinity is consistent with two NIDs in the same coactivator binding cooperatively to a single FXR-LBD subunit. However, another interpretation could be that the larger coactivator fragment is providing the energy for the dimerization of two FXR subunits. The crystal structure of PPAR γ in combination with an extended coactivator fragment (Nolte et al., 1998) shows the coactivator forming a bridge across the dimer interface of two LBDs. Therefore, we tested for the subunit dimerization of FXR-LBDs in the absence and presence of the NID (1-3) fragment (Figure 3E). Using gel filtration chromatography, we find that the FXR-LBD is monomeric in solution and that the addition of GRIP-1 NID (1-3) results in a complex consistent in size with a single subunit of FXR-LBD bound to a single NID (1-3) polypeptide. These results, together with the binding data in Figure 3D and the direct crystallographic observations shown in Figures 3A and 3B, are all consistent with a p160 coactivator forming its high-affinity interactions with an FXR-LBD by providing two LXXLL surfaces for the interaction.

Summary and Conclusions

The current structural study demonstrates a series of unanticipated findings associated with bile acid binding and activation of FXR. The bile acids are discerned from other steroids by their unusual physical shape and amphipathic properties. Bile acids occupy their pocket with their steroid nucleus positioned in the reverse orientation of all other steroids. This arrangement allows the distinctive *cis*-oriented ring A to impart the activated state to FXR by directly contacting a π -cation molecular switch deep in the pocket. The 3-OH group, which is conserved in all common bile acids, is not necessary for FXR activation. FXR is able to interact with a LXXLL motif that occupies the primary coactivator site, as well as a second motif that requires the agonist conformation of the receptor and further enhances the binding affinity of coactivator. Importantly, none of these features of FXR could have been predicted from structural studies thus far reported for other nuclear receptors.

Therapeutic bile acid supplementation has been a mainstay of Eastern medicine for centuries (Achord, 1990). More recently the bile acid UDCA has been used to treat cholestasis by displacement of more toxic bile acids from the enterohepatic pool (Hofmann, 1999b). However, UDCA is FXR silent and as such does not block *de novo* bile acid synthesis and has limited clinical efficacy. With the availability of these FXR structures, the potential exists to design new therapeutic bile acids with a modified balance of physicochemical and biological properties for treatment of cholestasis. In addition, the insights onto the molecular details of receptor activation should guide the development of nonsteroidal FXR modulators to impact hepatic cholesterol homeostasis, dietary cholesterol absorption, and serum triglycerides levels.

Experimental Procedures

Crystallization and Structure Determination

The ligand binding domain of rat FXR was subcloned into Nde1-BamH1 sites of pET16b vector (Novagen) and expressed with an N-terminal his-tag in BL21-DE3 *E. coli*. The cells were grown overnight in the presence of 0.5 mM IPTG. These cells were pelleted and frozen for long-term storage. For protein purification, the cells were thawed and sonicated in lysis buffer (400 mM NaCl, 10 mM imidazole, 10% glycerol, 20 mM Tris [pH 8.0]). The protein was purified using conventional Ni-NTA chromatography followed by loading on a 100 cm Superdex G200 column (Pharmacia). Ligand was added, and the protein concentration brought to 4–5 mg/ml by ultrafiltration followed by the addition of coactivator peptide. Crystals were grown in hanging drops by using polyethylene glycol as the precipitant, together with ethylene glycol (for cryoprotection) and 0.1M PIPES (pH 6.4). Crystals were flash frozen in liquid nitrogen, and the diffraction data were collected at beamline APS BM-19 in Argonne National Laboratory. Diffraction data were scaled and reduced with HKL2000 (Otwinowski and Minor, 1997). The structure of the 6ECDCA complex was solved using the molecular replacement with MOLREP (Vagin and Teplyakov, 1997). The search model consisted of the RAR LBD (PDB 1lbd) that was altered to remove most of the unconserved loops. The 3-deoxyCDCA structure was subsequently solved with molecular replacement using the refined 6ECDCA coordinates for the search model. Difference (Fo-Fc) maps calculated using phases derived from the 6ECDCA structure, but structure factors from the 3deoxyCDCA data clearly showed strong negative peaks corresponding to the 3-OH and 6-ethyl positions of the 3-deoxyCDCA, consistent with the differences in these ligands. Both structures were refined with multiple rounds of refinement with CNS (Brunger et al., 1998) followed by manual rebuilding.

Coactivator Binding Assays

The binding of coactivator peptides to FXR was measured using a fluorescence anisotropy-based assay with a Beacon 2000 (PanVera) system. Synthetic peptides were made at the University of Virginia Biomolecular Research Facility, corresponding to sequences shown in the Figure 3B legend. These peptides, as well as *E. coli*-expressed GRIP-1 NID (1-3) protein (sequence 563–767 of GRIP-1/SCR-2), were N-terminal fluorescein-labeled using previously described methods (Jacobs et al., 2001). To measure the K_D values for FXR-coactivator binding, the fluorescence anisotropy values of the peptides (50 nM concentrations) were measured in the presence of 2.5 mM bile acid concentrations and increasing FXR protein concentration. To determine EC_{50} values, the fluorescence anisotropy values of peptide (50 nM) were measured in the presence of FXR (0.1 mM) and increasing ligand concentrations. Data were fitted using the equation $A = [A_f - A_b][\text{protein}]/(K_D + [\text{protein}])$, where A_f and A_b are the anisotropy values of the free and bound peptides, respectively.

Acknowledgments

We thank Dr. C. Wright, Dr. W. Minor, and S. Jacobs (University of Virginia) for their helpful suggestions and assistance with the

Otwinowski, Z., and Minor, W. (1997). Processing of X-ray diffraction data collected in oscillation mode. *Methods Enzymol.* 276, 307–326.

Xu, L., Glass, C.K., and Rosenfeld, M.G. (1999). Coactivator and corepressor complexes in nuclear receptor function. *Curr. Opin. Genet. Dev.* 9, 140-147.

The Protein Data Bank code for the structure reported in this paper is 1OSV.